

Bacteriophage targeting of gut bacterium attenuates alcoholic liver disease

<https://doi.org/10.1038/s41586-019-1742-x>

Received: 9 April 2019

Accepted: 2 October 2019

Published online: 13 November 2019

Yi Duan^{1,2,29}, Cristina Llorente^{1,2,29}, Sonja Lang¹, Katharina Brandl³, Huikuan Chu¹, Lu Jiang^{1,2}, Richard C. White⁴, Thomas H. Clarke⁴, Kevin Nguyen⁴, Manolito Torralba⁵, Yan Shao⁶, Jinyuan Liu⁷, Adriana Hernandez-Morales⁸, Lauren Lessor⁹, Imran R. Rahman¹⁰, Yukiko Miyamoto¹, Melissa Ly¹¹, Bei Gao¹, Weizhong Sun¹, Roman Kiesel¹, Felix Huttmacher¹, Suhan Lee¹, Meritxell Ventura-Cots¹², Francisco Bosques-Padilla¹³, Elizabeth C. Verna¹⁴, Juan G. Abalde¹⁵, Robert S. Brown Jr¹⁶, Víctor Vargas^{17,18}, Jose Altamirano¹⁷, Juan Caballería^{18,19}, Debbie L. Shawcross²⁰, Samuel B. Ho^{1,2}, Alexandre Louvet²¹, Michael R. Lucey²², Philippe Mathurin²¹, Guadalupe Garcia-Tsao^{23,24}, Ramon Bataller¹², Xin M. Tu⁷, Lars Eckmann¹, Wilfred A. van der Donk^{10,25,26}, Ry Young^{8,9}, Trevor D. Lawley⁶, Peter Stärkel²⁷, David Pride^{1,11,28}, Derrick E. Fouts⁴ & Bernd Schnabl^{1,2,28*}

Chronic liver disease due to alcohol-use disorder contributes markedly to the global burden of disease and mortality^{1–3}. Alcoholic hepatitis is a severe and life-threatening form of alcohol-associated liver disease. The gut microbiota promotes ethanol-induced liver disease in mice⁴, but little is known about the microbial factors that are responsible for this process. Here we identify cytolysin—a two-subunit exotoxin that is secreted by *Enterococcus faecalis*^{5,6}—as a cause of hepatocyte death and liver injury. Compared with non-alcoholic individuals or patients with alcohol-use disorder, patients with alcoholic hepatitis have increased faecal numbers of *E. faecalis*. The presence of cytolysin-positive (cytolytic) *E. faecalis* correlated with the severity of liver disease and with mortality in patients with alcoholic hepatitis. Using humanized mice that were colonized with bacteria from the faeces of patients with alcoholic hepatitis, we investigated the therapeutic effects of bacteriophages that target cytolytic *E. faecalis*. We found that these bacteriophages decrease cytolysin in the liver and abolish ethanol-induced liver disease in humanized mice. Our findings link cytolytic *E. faecalis* with more severe clinical outcomes and increased mortality in patients with alcoholic hepatitis. We show that bacteriophages can specifically target cytolytic *E. faecalis*, which provides a method for precisely editing the intestinal microbiota. A clinical trial with a larger cohort is required to validate the relevance of our findings in humans, and to test whether this therapeutic approach is effective for patients with alcoholic hepatitis.

The most severe form of alcohol-related liver disease is alcoholic hepatitis; mortality ranges from 20% to 40% at 1–6 months, and as many as 75% of patients die within 90 days of a diagnosis of severe alcoholic hepatitis^{7–9}. Therapy with corticosteroids is only marginally effective⁹. Early liver transplantation is the only curative therapy, but is offered only at select centres and to a limited group of patients¹⁰.

Alcohol-related liver disease can be transmitted via faecal microbiota⁴. We investigated the microorganisms and microbial factors that are responsible for this transmissible phenotype and for progression of alcohol-related liver disease.

Cytolysin linked to increased mortality

We performed 16S ribosomal RNA (rRNA) gene sequencing to determine whether chronic alcohol use and alcoholic hepatitis are associated

with an altered composition of the faecal microbiota. Differences in faecal microbiota composition were noted in patients with alcohol-use disorder and alcoholic hepatitis, compared to subjects without alcohol-use disorder (controls) (Fig. 1a, Extended Data Fig. 1a, b, Supplementary Tables 1, 2). One substantial difference that we observed was an increase in the proportion of *Enterococcus* spp. in patients with alcoholic hepatitis: in these patients, 5.59% of faecal bacteria were *Enterococcus* spp. compared with almost none in controls (0.023%; for comparison, 0.004% of all reads were *Enterococcus* spp. in the Human Microbiome Project) or patients with alcohol-use disorder (0.024%). Faecal samples from patients with alcoholic hepatitis had about 2,700-fold more *E. faecalis* than samples from controls, as measured by quantitative PCR (qPCR) (Extended Data Fig. 1c), which is consistent with the 16S rRNA sequencing results. About 80% of patients with alcoholic hepatitis are positive for *E. faecalis* in their faeces (Extended Data Fig. 1d).

A list of affiliations appears at the end of the paper.

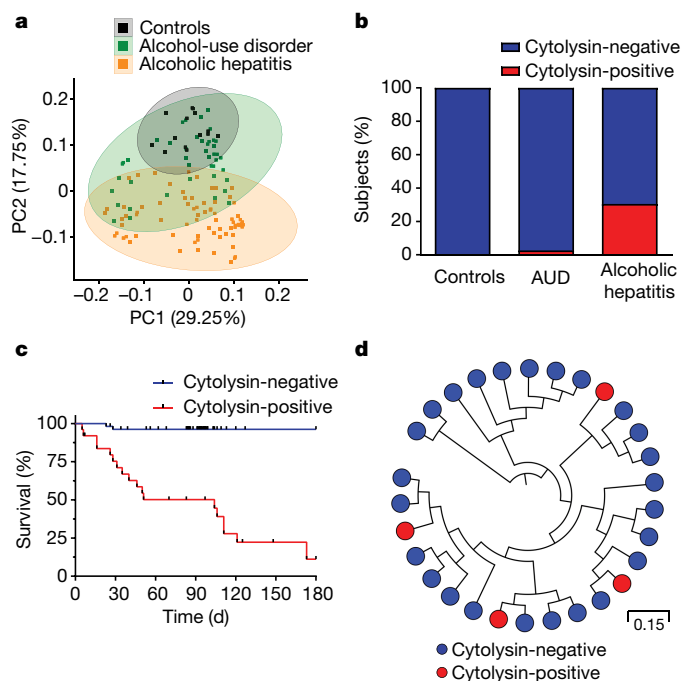


Fig. 1 | *E. faecalis* cytolyisin is associated with mortality in patients with alcoholic hepatitis. **a**, 16S rRNA sequencing of faecal samples from controls ($n=14$), patients with alcohol-use disorder ($n=43$) or alcoholic hepatitis ($n=75$). We use principal coordinate analysis (PCoA) based on Jaccard dissimilarity matrices to show β -diversity among groups at the genus level. The composition of faecal microbiota was significantly different between each group ($P < 0.01$). **b**, Percentage of subjects with faecal samples that were positive for both *cytL₁* and *cytL₅* DNA sequences (cytolyisin-positive), in controls ($n=25$), patients with alcohol-use disorder ($n=38$) or alcoholic hepatitis ($n=82$), assessed by qPCR. Statistically significant differences were detected between controls and patients with alcoholic hepatitis ($P < 0.01$), and between patients with alcohol-use disorder and patients with alcoholic hepatitis ($P < 0.001$). **c**, Kaplan–Meier curve of survival of patients with alcoholic hepatitis whose faecal samples were cytolyisin-positive ($n=25$) or cytolyisin-negative ($n=54$) ($P < 0.0001$). **d**, Core genome single-nucleotide polymorphism (SNP) tree of *E. faecalis* strains isolated from patients with alcoholic hepatitis ($n=93$ strains, from 24 patients), showing phylogenetic diversity of cytolyisin-positive (red) *E. faecalis*. Genomically identical isolates from the same patient were combined, and are shown as a single dot. Scale bar represents the nucleotide substitutions per SNP site. P values are determined by permutational multivariate analysis of variance (PERMANOVA) followed by false discovery rate (FDR) procedures (**a**), two-sided Fisher's exact test followed by FDR procedures (**b**) or two-sided log-rank (Mantel–Cox) test (**c**). The exact group size (n) and P values for each comparison are listed in Supplementary Table 10.

The colonization of mice with *E. faecalis* induces mild hepatic steatosis and exacerbates ethanol-induced liver disease¹¹, by mechanisms that are unclear. Cytolyisin is a bacterial exotoxin (or bacteriocin) that is produced by *E. faecalis*¹², and which contains two post-translationally modified peptides (CytL₁' and CytL₅'') in its bioactive form⁶. The two peptides are encoded by two separate genes: *cytL₁* and *cytL₅*, respectively¹². Cytolyisin has lytic activity against not only Gram-positive bacteria, but also eukaryotic cells¹³. We detected *cytL₁* and *cytL₅* genomic DNA (cytolyisin-positive) in faecal samples from 30% of patients with alcoholic hepatitis; none of the faecal samples from controls and only one sample from a patient with alcohol-use disorder was cytolyisin-positive, as detected by qPCR (Fig. 1b). Importantly, 89% of cytolyisin-positive patients with alcoholic hepatitis died within 180 days of admission, compared to only 3.8% of cytolyisin-negative patients ($P < 0.0001$) (Fig. 1c). Among the cytolyisin-positive patients, 72.2% (13 out of 18) died owing to liver failure (including complications related to liver

failure, such as gastrointestinal bleeding) (Supplementary Table 2). Infection was not associated with 30-day, 90-day or 180-day mortality ($P = 0.403, 0.234$ or 0.098) in patients with alcoholic hepatitis.

Our univariate logistic and Cox regression of laboratory and clinical parameters found an association between the detection of cytolyisin-encoding genes in faeces and the international normalized ratio (INR), platelet count, the model for end-stage liver disease (MELD) score, the sodium MELD score, the age, serum bilirubin, INR and serum creatinine (ABIC) score and death (Supplementary Table 3). In the multivariate Cox analysis, detection of cytolyisin-encoding genes in faeces was associated with 90-day ($P = 0.004$) and with 180-day mortality ($P = 0.001$) (Supplementary Table 3), even after we adjusted for the geographical origin of the patient, antibiotic treatment, platelet count, and creatinine, bilirubin and INR as components of the MELD score. We found no multicollinearity between the detection of faecal cytolyisin-encoding genes and these cofactors (variance inflation factor < 1.6), which indicates that cytolyisin is an independent predictor of mortality in patients with alcoholic hepatitis. When we performed receiver-operating-characteristic curve analysis for 90-day mortality, cytolyisin had an area under the curve of 0.81, which was superior to other widely used predictors for mortality in clinical practice (Extended Data Fig. 1e). On the basis of our findings, we propose that the detection of cytolyisin may be a prognostic factor for more severe liver-related outcomes and increased risk of death, and a stronger predictor of mortality than MELD, ABIC and the discriminant function score.

To determine phylogeny of *E. faecalis* in patients with alcoholic hepatitis, we performed targeted culturing from stool samples. Whole-genome sequencing of 93 *E. faecalis* isolates revealed a broad phylogenetic diversity of cytolyisin-positive *E. faecalis* from patients with alcoholic hepatitis (Fig. 1d), which indicates that cytolyisin production is a variable trait among *E. faecalis* isolates and that cytolyisin is carried in mobile genetic elements, which include both chromosomally encoded pathogenicity islands and plasmids¹⁴. Detection of any other antimicrobial resistance genes or virulence genes in *E. faecalis* isolates did not correlate with disease severity or mortality in patients with alcoholic hepatitis (Supplementary Table 4).

The total amount of faecal *E. faecalis*, or faecal *E. faecalis* positivity, did not correlate with disease severity or mortality in patients with alcoholic hepatitis (Supplementary Tables 5, 6). Cytolyisin-positive and cytolyisin-negative patients with alcoholic hepatitis had similar amounts of faecal *E. faecalis* (Extended Data Fig. 1f). Although there were differences in the composition of the gut microbiota in patients with alcoholic hepatitis from different geographical regions (Extended Data Fig. 1g), the proportion of cytolyisin-positive patients, total amount of faecal *E. faecalis*, faecal *E. faecalis* positivity (Extended Data Fig. 1h–j), treatment and clinical outcomes (30-day and 90-day mortality) did not differ significantly among the regions or centres (Supplementary Table 7). In addition, cirrhosis was not associated with cytolyisin positivity, the total amount of faecal *E. faecalis* or faecal *E. faecalis* positivity in patients with alcoholic hepatitis (Extended Data Fig. 1k–m, Supplementary Tables 4–6). These results confirm our findings that the presence of cytolyisin-producing *E. faecalis* rather than the total amount or presence of *E. faecalis* per se determines the severity of alcoholic hepatitis and mortality.

Cytolyisin and ethanol-induced liver disease

To determine whether cytolyisin contributes to liver damage mediated by *E. faecalis*, we gavaged mice with a cytolytic *E. faecalis* strain (FA2-2(pAM714)) or a non-cytolytic *E. faecalis* strain (FA2-2(pAM771))⁵; the mice were then placed on a chronic–binge ethanol diet¹⁵. Compared to mice gavaged with phosphate-buffered saline (PBS), mice fed with ethanol after they were gavaged with cytolytic *E. faecalis* developed more severe liver injury as indicated by a higher level of alanine aminotransferase (ALT) (Extended Data Fig. 2a) and increased hepatic steatosis (Extended Data Fig. 2b, c). Mice that were fed ethanol after they

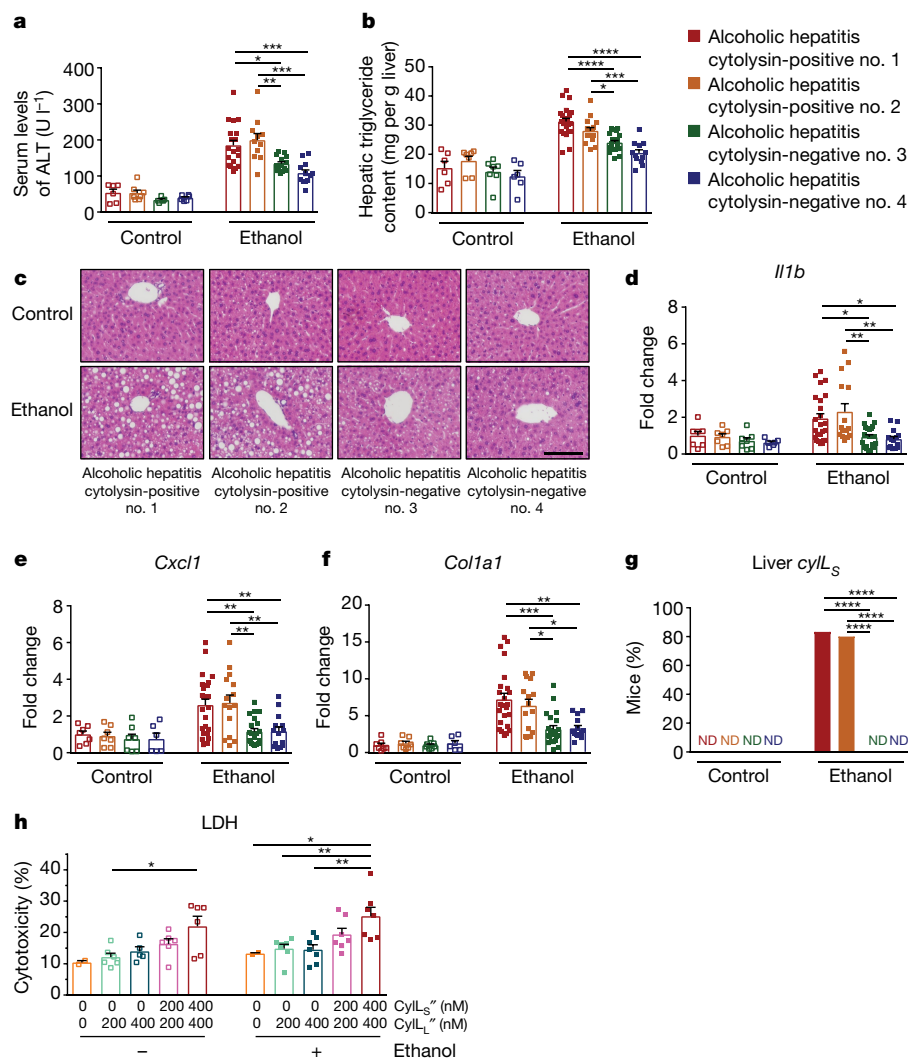


Fig. 2 | Transplantation of faeces from cytolysin-positive patients with alcoholic hepatitis exacerbates ethanol-induced liver disease in gnotobiotic mice. **a–g**, C57BL/6 germ-free mice were colonized with faeces from two cytolysin-positive and two cytolysin-negative patients with alcoholic hepatitis, and subjected to the chronic–binge feeding model. **a**, Serum levels of ALT. **b**, Hepatic triglyceride content. **c**, Representative sections of liver stained with haematoxylin and eosin (H & E). **d–f**, Hepatic levels of mRNAs that encode *I11b*, *Cxcl1* and *Col1a1*. **g**, Proportions of mice that were positive for cytolysin in the liver, measured by qPCR for *cyll_s*. **h**, Lactate dehydrogenase (LDH) assay to measure cytotoxicity of hepatocytes isolated from mice that were fed an oral isocaloric control diet (five groups, left) or chronic–binge ethanol diet (five

groups, right), and incubated with vehicle, *CyLL_s*, *CyLL_L* or both of the cytolysin subunits at the indicated concentrations without (–) or with (+) ethanol (25 mM) for 3 h. The survival of hepatocytes was determined in three independent experiments. Scale bar, 100 μ m. Results are expressed as mean \pm s.e.m. (**a**, **b**, **d–f**, **h**). *P* values are determined by one-way analysis of variance (ANOVA) with Tukey’s post hoc test (**a**, **b**, **d–f**), two-sided Fisher’s exact test followed by FDR procedures (**g**) or two-way ANOVA with Tukey’s post hoc test (**h**). All results were generated from at least three independent replicates. The exact group size (*n*) and *P* values for each comparison are listed in Supplementary Table 10. **P* < 0.05, ***P* < 0.01, ****P* < 0.001, *****P* < 0.0001.

were gavaged with cytolysin *E. faecalis* also had more liver inflammation with higher expression levels of mRNAs that encode inflammatory cytokines and chemokines (*I11b*, *Cxcl1* and *Cxcl2*) (Extended Data Fig. 2d–f), compared with mice given PBS. Mice that were fed ethanol after they were gavaged with non-cytolytic *E. faecalis* had significantly less ethanol-induced liver injury, steatosis and inflammation (Extended Data Fig. 2a–f) and longer survival times (Extended Data Fig. 2g), as compared with mice that were fed ethanol after they were administered with cytolysin *E. faecalis*.

To explore the mechanism of cytolysin-associated liver damage, we measured cytolysin in the liver. *CyLL_s* was significantly increased in the liver of mice given cytolysin *E. faecalis* but not in the liver of mice that were not given *E. faecalis* or of mice gavaged with non-cytolytic *E. faecalis* after chronic ethanol administration (Extended Data Fig. 2h). *E. faecalis* was detectable in the liver of mice given cytolysin and

non-cytolytic *E. faecalis* and fed an ethanol diet, but not when mice were fed an isocaloric (control) diet (Extended Data Fig. 2i); this indicates that ethanol-induced changes in the gut barrier are necessary for the translocation of cytolysin *E. faecalis* from the intestine to the liver. The livers of ethanol-fed mice that were given cytolysin or non-cytolytic *E. faecalis* had positive *E. faecalis* cultures (Extended Data Fig. 2j). We observed an increased intestinal permeability in ethanol-fed mice compared with mice fed with an isocaloric diet, but this was independent of gavaging cytolysin or non-cytolytic *E. faecalis* after chronic ethanol administration (Extended Data Fig. 2k), indicating that cytolysin does not affect intestinal barrier function.

Administration of cytolysin or non-cytolytic *E. faecalis* to mice did not significantly change the composition of the intestinal microbiota, as shown by 16S rRNA gene sequencing (Extended Data Fig. 2l). Cytolysin *E. faecalis* did not affect intestinal absorption or hepatic metabolism

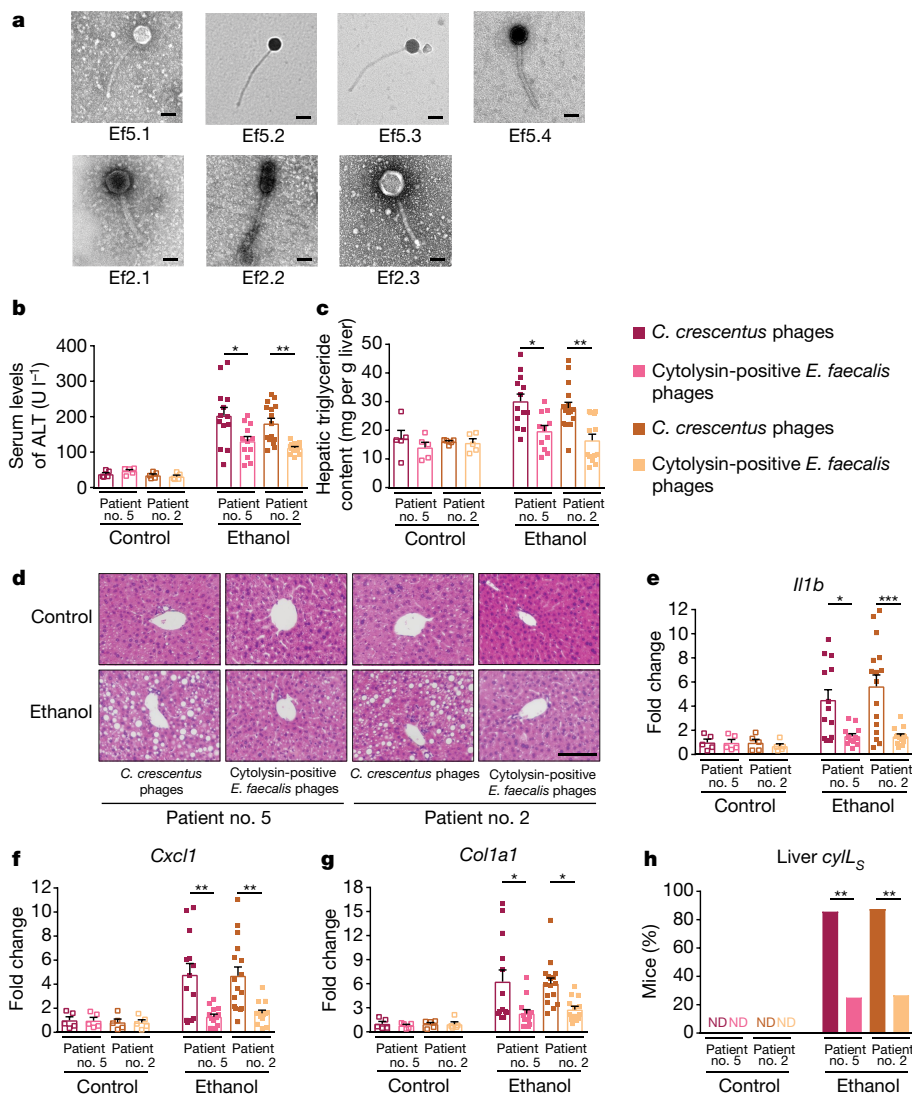


Fig. 3 | Phage therapy against cytolytic *E. faecalis* abolishes ethanol-induced liver disease in gnotobiotic mice. **a**, Transmission electron microscopy revealed that the phages we isolated were either siphophages (Ef5.1, Ef5.2, Ef5.3, Ef5.4 and Ef2.2) or myophages (Ef2.1 and Ef2.3). Scale bar, 50 nm. **b–h**, C57BL/6 germ-free mice were colonized with faeces from two cytolytin-positive patients with alcoholic hepatitis (faeces from one of these patients were also used in Fig. 2) and subjected to the chronic–binge feeding model, gavaged with control phages against *C. crescentus* (10^{10} plaque-forming units (PFUs)) or a cocktail of three or four different phages that target cytolytic *E. faecalis* (10^{10} PFUs), 1 day before an ethanol binge. **b**, Serum levels of ALT.

c, Hepatic triglyceride content. **d**, Representative H & E-stained liver sections. Scale bar, 100 μ m. **e–g**, Hepatic levels of mRNAs that encode *I11b*, *Cxcl1* and *Col1a1*. **h**, Proportions of mice that were positive for cytolytin in the liver, measured by qPCR for *cyLL_S*. Results are expressed as mean \pm s.e.m. (**b**, **c**, **e–g**). *P* values are determined by two-way ANOVA with Tukey’s post hoc test (**b**, **c**, **e–g**) or two-sided Fisher’s exact test followed by FDR procedures (**h**). All results are generated from at least three independent replicates. The exact group size (*n*) and *P* values for each comparison are listed in Supplementary Table 10. **P* < 0.05, ***P* < 0.01, ****P* < 0.001.

of ethanol, as indicated by serum levels of ethanol and hepatic levels of *Adh1* and *Cyp2e1* mRNAs (which encode the two primary enzymes that metabolize ethanol in the liver) (Extended Data Fig. 2m, n). These results indicate that *E. faecalis* that produce cytolytin promote ethanol-induced liver disease in mice.

To extend our findings to humans, we colonized germ-free mice with faeces from cytolytin-positive and cytolytin-negative patients with alcoholic hepatitis (Supplementary Table 8). Consistent with our findings from mice colonized with cytolytic *E. faecalis*, gnotobiotic C57BL/6 mice colonized with faeces from two cytolytin-positive patients developed more severe ethanol-induced liver injury, steatosis, inflammation and fibrosis than mice given faeces from two cytolytin-negative patients (Fig. 2a–f, Extended Data Fig. 3a–d). Transplantation of faeces from cytolytin-positive patients reduced the survival time of the mice (Extended Data Fig. 3e) and increased translocation of

cytolytic *E. faecalis* to the liver after ethanol administration (Fig. 2g). The overall composition of the intestinal microbiota was not different between mice fed the control diet and colonized with faeces from cytolytin-positive or cytolytin-negative donors with alcoholic hepatitis, as shown by 16S rRNA gene sequencing. Mice transplanted with faeces from one of the cytolytin-positive patients with alcoholic hepatitis (patient no. 2) showed a microbiota that was significantly different from that of the other mouse groups after ethanol administration (Extended Data Fig. 3f). Non-cytolytic *E. faecalis* was not detected in stool samples from donors with cytolytic *E. faecalis* (Extended Data Fig. 3g). We did not observe differences in intestinal absorption or hepatic metabolism of ethanol between mice colonized with faeces from cytolytin-positive versus cytolytin-negative patients (Extended Data Fig. 3h, i). Together, these results provide further evidence that cytolytin promotes ethanol-induced liver disease.

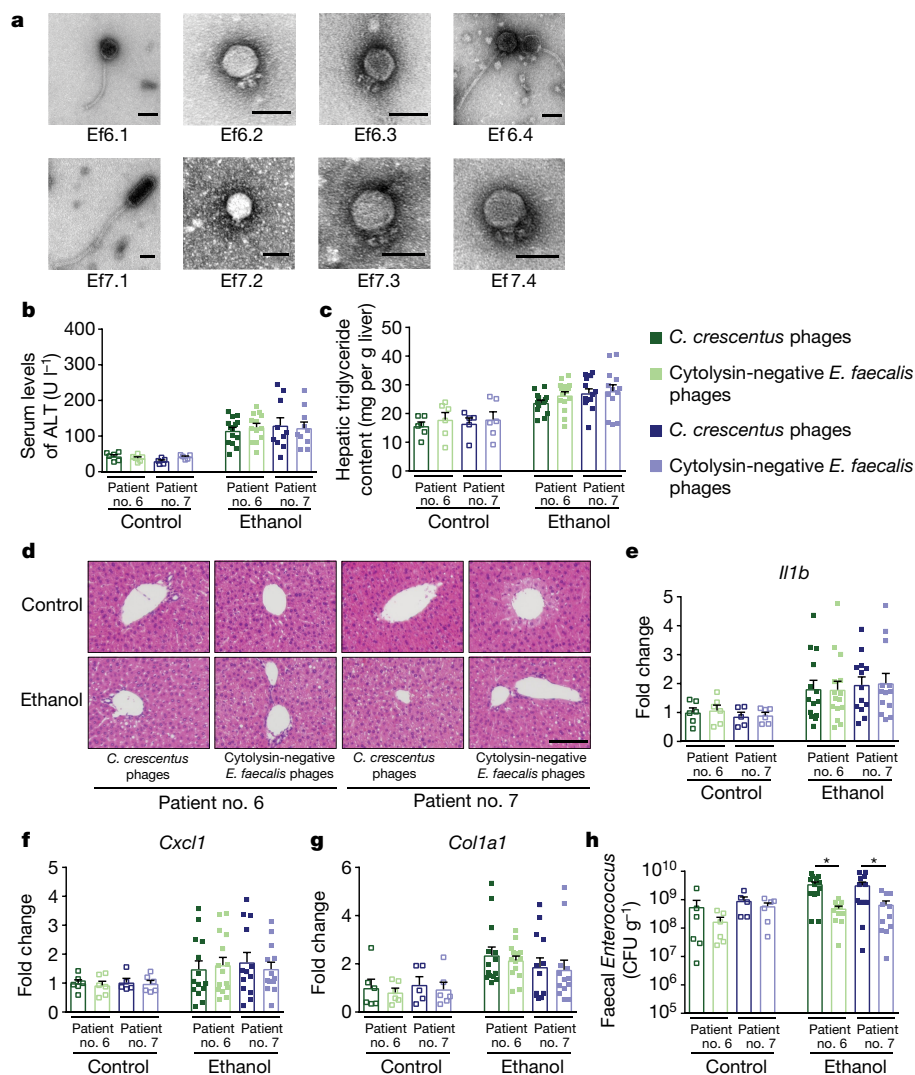


Fig. 4 | Phages that target non-cytolytic *E. faecalis* do not reduce ethanol-induced liver disease in gnotobiotic mice. a, Transmission electron microscopy revealed that the phages we isolated were either podophages (Ef6.2, Ef6.3, Ef7.2, Ef7.3 and Ef7.4) or siphophages (Ef6.1, Ef6.4 and Ef7.1). Scale bar, 50 nm. **b–h**, C57BL/6 germ-free mice were colonized with faeces from two cytolysin-negative patients with alcoholic hepatitis and subjected to the chronic–binge feeding model, gavaged with control phages against *C. crescentus* (10^{10} PFUs) or a cocktail of four different phages that target non-

cytolytic *E. faecalis* (10^{10} PFUs), 1 day before an ethanol binge. **b**, Serum levels of ALT. **c**, Hepatic triglyceride content. **d**, Representative H & E-stained liver sections. Scale bar, 100 μ m. **e–g**, Hepatic levels of mRNAs that encode *Il1b*, *Cxcl1* and *Col1a1*. **h**, Faecal colony-forming units (CFUs) of *Enterococcus*. Results are expressed as mean \pm s.e.m. (**b**, **c**, **e–h**). *P* values are determined by two-way ANOVA with Tukey’s post hoc test (**b**, **c**, **e–h**). All results were generated from at least three independent replicates. The exact group size (*n*) and *P* values for each comparison are listed in Supplementary Table 10. **P* < 0.05.

To determine the mechanism by which cytolysin increases liver disease, we isolated hepatocytes from mice fed ethanol or control diets, and stimulated them with pure bioactive cytolysin peptides (CylL_L’ and CylL_S’)⁶. Incubation of the primary mouse hepatocytes with the two cytolysin subunits caused a dose-dependent increase in cell death compared to hepatocytes that were incubated with vehicle or with one subunit only (Fig. 2h). When we isolated hepatocytes from ethanol-fed mice and then incubated these hepatocytes with ethanol, we did not observe increased levels of cytolysin-induced cell death compared to hepatocytes isolated from mice on the control diet, which indicates that cytolysin-induced hepatocyte cell death was independent of ethanol. The cytotoxic effects of cytolysin are possibly mediated by pore formation, resulting in cell lysis¹⁴.

Bacteriophage treatment in liver disease

To further demonstrate the potential causative role of cytolytic *E. faecalis* for the development of ethanol-induced steatohepatitis,

we investigated the effects of treatment with bacteriophages (hereafter, phages). Phages are ubiquitous in bacteria-rich environments, including the gut¹⁶. *E. faecalis* phages that are highly strain-specific can be isolated¹⁷, which potentially makes the direct editing of gut microbiota feasible. It has previously been shown that *Atp4a*^{SI/SI} mice, which lack gastric acid, have overgrowth of intestinal enterococci, which is associated with increased susceptibility to alcohol-induced steatohepatitis¹¹. The gavaging of wild-type mice with an *E. faecalis* strain isolated from *Atp4a*^{SI/SI} mice led to increased ethanol-induced steatohepatitis¹¹. We found that this same *E. faecalis* strain expressed cytolysin. We then isolated four distinct phages from sewage water. These phages lyse the cytolytic *E. faecalis* strain isolated from *Atp4a*^{SI/SI} mice. All four phages were podophages of the virulent *Picovirinae* group (Extended Data Fig. 4). *Atp4a*^{SI/SI} mice and their wild-type littermates were then placed on the chronic–binge ethanol diet and gavaged with the lytic phage cocktail. Phages directed against *Caulobacter crescentus*, a bacterium that is present in freshwater lakes and streams¹⁸ but that does not colonize humans or rodents^{19,20}, were used as controls.

Compared to *Atp4a*^{sl/sl} mice gavaged with control phages or vehicle, *Atp4a*^{sl/sl} mice gavaged with phages that target cytolysin *E. faecalis* had less severe liver injury, steatosis and inflammation after chronic ethanol feeding (Extended Data Fig. 5a–f). Administration of *E. faecalis* phages significantly reduced levels of cytolysin in the liver (Extended Data Fig. 5g) as well as faecal amounts of *Enterococcus* (Extended Data Fig. 5h). Phage administration did not affect the overall composition of the faecal microbiome, intestinal absorption or hepatic metabolism of ethanol (Extended Data Fig. 5i–k).

To develop a therapeutic approach to precisely edit the intestinal microbiota, we cultured cytolysin *E. faecalis* strains from the faecal samples of patients with alcoholic hepatitis. We then isolated lytic phages from sewage water against these cytolysin *E. faecalis* strains; these phages had siphophage or myophage morphology (Fig. 3a, Extended Data Fig. 6). Gnotobiotic mice were colonized with faeces from two cytolysin-positive patients with alcoholic hepatitis (Supplementary Table 8) and given three or four different—but patient-specific—lytic phages against cytolysin *E. faecalis*. The phages against cytolysin *E. faecalis* abolished ethanol-induced liver injury and steatosis, as shown by lower levels of ALT, lower percentages of hepatic cells positive for terminal deoxynucleotide transferase-mediated dUTP nick-end labelling, and lower levels of hepatic triglycerides and oil red O-staining (Fig. 3b–d, Extended Data Fig. 7a, b), as well as by decreased hepatic levels of *Il1b*, *Cxcl1*, *Cxcl2*, *Col1a1* and *Acta2* mRNAs, and reduced hepatic levels of *cytL*_s, as compared with mice given control phages (against *C. crescentus*) (Fig. 3e–h, Extended Data Fig. 7c, d). Treatment with phages against cytolysin *E. faecalis* also reduced faecal amounts of *Enterococcus* (Extended Data Fig. 7e) without affecting the overall composition of the gut microbiota (Extended Data Fig. 7f). Intestinal absorption of ethanol and hepatic metabolism were similar in all groups (Extended Data Fig. 7g, h).

To demonstrate that the effect of phage treatment occurs via the targeting of cytolysin-positive *E. faecalis*, rather than a reduction in cytolysin-negative *E. faecalis*, we colonized gnotobiotic mice with faeces from cytolysin-negative patients with alcoholic hepatitis (Supplementary Table 8). Phages against non-cytolysin *E. faecalis* from patients were isolated from sewage water; they had siphophage or podophage morphology (Fig. 4a, Extended Data Fig. 8). These phages did not reduce features of ethanol-induced liver disease compared with control phages (Fig. 4b–g, Extended Data Fig. 9a–h), despite the reduction of faecal *Enterococcus* (Fig. 4h). Our findings indicate that treatment with lytic phages can selectively attenuate the ethanol-induced liver disease caused by cytolysin-positive *E. faecalis* in humanized mice.

Discussion

Phage-based therapies have predominantly been studied in patients with bacterial infections in the gastrointestinal tract^{21–23}, urinary tract^{24,25} and other organ systems^{26–28}. The results of these studies—although mixed in terms of efficacy—strongly suggest that phage treatment offers a safe alternative to antibiotics^{26,27}. However, safety studies are required for complex populations (such as patients with alcoholic hepatitis), because phages can induce a strong immune reaction²⁹. Further work is required to determine whether phages that target cytolysin *E. faecalis* might be used to treat patients with alcoholic hepatitis, a life-threatening disease that at present has no effective treatment. Eradication of this specific bacterial strain might produce better outcomes than current treatments, and environmental sources can be used to easily isolate phages that target cytolysin-positive *E. faecalis*. Here we provide an example of the efficacy of approaches based on phages in mice for a disease that is not considered a classic infectious disease. Our data also suggest that cytolysin may be used as a predictive biomarker of severe alcoholic hepatitis; an independent, prospective

cohort is therefore needed to validate cytolysin as a biomarker, and to extend the phage findings in mice to human patients.

Online content

Any methods, additional references, Nature Research reporting summaries, source data, extended data, supplementary information, acknowledgements, peer review information; details of author contributions and competing interests; and statements of data and code availability are available at <https://doi.org/10.1038/s41586-019-1742-x>.

- Lozano, R. et al. Global and regional mortality from 235 causes of death for 20 age groups in 1990 and 2010: a systematic analysis for the Global Burden of Disease Study 2010. *Lancet* **380**, 2095–2128 (2012).
- Lee, B. P., Vittinghoff, E., Dodge, J. L., Cullaro, G. & Terrault, N. A. National trends and long-term outcomes of liver transplant for alcohol-associated liver disease in the United States. *JAMA Intern. Med.* **179**, 340–348 (2019).
- Rehm, J. et al. Burden of disease associated with alcohol use disorders in the United States. *Alcohol. Clin. Exp. Res.* **38**, 1068–1077 (2014).
- Llopis, M. et al. Intestinal microbiota contributes to individual susceptibility to alcoholic liver disease. *Gut* **65**, 830–839 (2016).
- Ike, Y., Clewell, D. B., Segarra, R. A. & Gilmore, M. S. Genetic analysis of the pAD1 hemolysin/bacteriocin determinant in *Enterococcus faecalis*: Tn917 insertional mutagenesis and cloning. *J. Bacteriol.* **172**, 155–163 (1990).
- Tang, W. & van der Donk, W. A. The sequence of the enterococcal cytolysin imparts unusual lanthionine stereochemistry. *Nat. Chem. Biol.* **9**, 157–159 (2013).
- Maddrey, W. C. et al. Corticosteroid therapy of alcoholic hepatitis. *Gastroenterology* **75**, 193–199 (1978).
- Dominguez, M. et al. A new scoring system for prognostic stratification of patients with alcoholic hepatitis. *Am. J. Gastroenterol.* **103**, 2747–2756 (2008).
- Thursz, M. R. et al. Prednisolone or pentoxifylline for alcoholic hepatitis. *N. Engl. J. Med.* **372**, 1619–1628 (2015).
- Mathurin, P. & Lucey, M. R. Management of alcoholic hepatitis. *J. Hepatol.* **56**, S39–S45 (2012).
- Llorente, C. et al. Gastric acid suppression promotes alcoholic liver disease by inducing overgrowth of intestinal *Enterococcus*. *Nat. Commun.* **8**, 837 (2017).
- Gilmore, M. S. et al. Genetic structure of the *Enterococcus faecalis* plasmid pAD1-encoded cytolysin toxin system and its relationship to lantibiotic determinants. *J. Bacteriol.* **176**, 7335–7344 (1994).
- Cox, C. R., Coburn, P. S. & Gilmore, M. S. Enterococcal cytolysin: a novel two component peptide system that serves as a bacterial defense against eukaryotic and prokaryotic cells. *Curr. Protein Pept. Sci.* **6**, 77–84 (2005).
- Van Tyne, D., Martin, M. J. & Gilmore, M. S. Structure, function, and biology of the *Enterococcus faecalis* cytolysin. *Toxins* **5**, 895–911 (2013).
- Bertola, A., Mathews, S., Ki, S. H., Wang, H. & Gao, B. Mouse model of chronic and binge ethanol feeding (the NIAAA model). *Nat. Protoc.* **8**, 627–637 (2013).
- Ogilvie, L. A. & Jones, B. V. The human gut virome: a multifaceted majority. *Front. Microbiol.* **6**, 918 (2015).
- Chatterjee, A. et al. Bacteriophage resistance alters antibiotic-mediated intestinal expansion of enterococci. *Infect. Immun.* **87**, e00085-19 (2019).
- Poindexter, J. S. Biological properties and classification of the *Caulobacter* group. *Bacteriol. Rev.* **28**, 231–295 (1964).
- Shin, J. et al. Analysis of the mouse gut microbiome using full-length 16S rRNA amplicon sequencing. *Sci. Rep.* **6**, 29681 (2016).
- Human Microbiome Project Consortium. Structure, function and diversity of the healthy human microbiome. *Nature* **486**, 207–214 (2012).
- Marcuk, L. M. et al. Clinical studies of the use of bacteriophage in the treatment of cholera. *Bull. World Health Organ.* **45**, 77–83 (1971).
- Sarker, S. A. et al. Oral phage therapy of acute bacterial diarrhea with two coliphage preparations: a randomized trial in children from Bangladesh. *EBioMedicine* **4**, 124–137 (2016).
- Dalmaso, M., Hill, C. & Ross, R. P. Exploiting gut bacteriophages for human health. *Trends Microbiol.* **22**, 399–405 (2014).
- Ujmajuridze, A. et al. Adapted bacteriophages for treating urinary tract infections. *Front. Microbiol.* **9**, 1832 (2018).
- Khawaldeh, A. et al. Bacteriophage therapy for refractory *Pseudomonas aeruginosa* urinary tract infection. *J. Med. Microbiol.* **60**, 1697–1700 (2011).
- Schooley, R. T. et al. Development and use of personalized bacteriophage-based therapeutic cocktails to treat a patient with a disseminated resistant *Acinetobacter baumannii* infection. *Antimicrob. Agents Chemother.* **61**, e00954-17 (2017).
- Dedrick, R. M. et al. Engineered bacteriophages for treatment of a patient with a disseminated drug-resistant *Mycobacterium abscessus*. *Nat. Med.* **25**, 730–733 (2019).
- Fish, R. et al. Compassionate use of bacteriophage therapy for foot ulcer treatment as an effective step for moving toward clinical trials. *Methods Mol. Biol.* **1693**, 159–170 (2018).
- Górski, A. et al. Phages and immunomodulation. *Future Microbiol.* **12**, 905–914 (2017).

Publisher's note Springer Nature remains neutral with regard to jurisdictional claims in published maps and institutional affiliations.

© The Author(s), under exclusive licence to Springer Nature Limited 2019

¹Department of Medicine, University of California San Diego, La Jolla, CA, USA. ²Department of Medicine, VA San Diego Healthcare System, San Diego, CA, USA. ³Skaggs School of Pharmacy and Pharmaceutical Sciences, University of California San Diego, La Jolla, CA, USA. ⁴J. Craig Venter Institute, Rockville, MD, USA. ⁵J. Craig Venter Institute, La Jolla, CA, USA. ⁶Host–Microbiota Interactions Laboratory, Wellcome Sanger Institute, Hinxton, UK. ⁷Division of Biostatistics and Bioinformatics, Department of Family Medicine and Public Health, University of California San Diego, La Jolla, CA, USA. ⁸Department of Biochemistry and Biophysics, Texas A & M University, College Station, TX, USA. ⁹Center for Phage Technology, Texas A & M AgriLife Research and Texas A & M University, College Station, TX, USA. ¹⁰Department of Biochemistry, University of Illinois at Urbana-Champaign, Urbana, IL, USA. ¹¹Department of Pathology, University of California San Diego, La Jolla, CA, USA. ¹²Division of Gastroenterology, Hepatology and Nutrition, Department of Medicine, University of Pittsburgh Medical Center, Pittsburgh Liver Research Center, Pittsburgh, PA, USA. ¹³Hospital Universitario, Departamento de Gastroenterología, Universidad Autónoma de Nuevo Leon, Monterrey, Mexico. ¹⁴Division of Digestive and Liver Diseases, Department of Medicine, Columbia University College of Physicians and Surgeons, New York, NY, USA. ¹⁵Department of Medicine, University of Alberta, Edmonton, Alberta, Canada. ¹⁶Division of

Gastroenterology and Hepatology, Weill Cornell Medical College, New York, NY, USA. ¹⁷Liver Unit, Hospital Universitari Vall d'Hebron, Universitat Autònoma de Barcelona, Barcelona, Spain. ¹⁸Centro de Investigación en Red de Enfermedades Hepáticas y Digestivas (CIBEREHD), Barcelona, Spain. ¹⁹Liver Unit, Hospital Clinic, Barcelona, Spain. ²⁰Liver Sciences, Department of Inflammation Biology, School of Infectious Diseases and Microbial Sciences, King's College London, London, UK. ²¹Service des Maladies de L'appareil Digestif et Unité INSERM, Hôpital Huriez, Lille, France. ²²Division of Gastroenterology and Hepatology, Department of Medicine, University of Wisconsin School of Medicine and Public Health, Madison, WI, USA. ²³Section of Digestive Diseases, Yale University School of Medicine, New Haven, CT, USA. ²⁴Section of Digestive Diseases, VA Connecticut Healthcare System, West Haven, CT, USA. ²⁵Department of Chemistry, University of Illinois at Urbana-Champaign, Urbana, IL, USA. ²⁶Howard Hughes Medical Institute, University of Illinois at Urbana-Champaign, Urbana, IL, USA. ²⁷St Luc University Hospital, Université Catholique de Louvain, Brussels, Belgium. ²⁸Center for Innovative Phage Applications and Therapeutics, University of California San Diego, La Jolla, CA, USA. ²⁹These authors contributed equally: Yi Duan, Cristina Llorente. *e-mail: beschnabl@ucsd.edu

Article

Methods

No statistical methods were used to predetermine sample size. The experiments were not randomized and investigators were not blinded to allocation during experiments and outcome assessment.

Patient cohorts

Patient cohorts have previously been described^{30–32}. We evaluated 26 subjects without alcohol-use disorder (controls; social drinkers consuming less than 20 g/day), 44 patients with alcohol-use disorder and 88 patients with alcoholic hepatitis. Patients with alcohol-use disorder fulfilling the DSM IV criteria³³ of alcohol dependence and with active alcohol consumption (self-reported >60 g/day) presented with various stages of liver disease (21% had advanced F3/4 fibrosis based on fibrosis-4 index) (Supplementary Table 1). Patients with alcohol-use disorder were recruited from an alcohol withdrawal unit in San Diego and Brussels, where they followed a detoxification and rehabilitation programme. At admission to the hospital, a complete medication and medical history was taken, and a complete physical examination was performed, including collection of bio-specimens, basic demographic data (such as age, gender, weight and height) and self-reported daily alcohol consumption. Patients were actively drinking until the day of admission. Controls or patients with alcohol-use disorder did not take antibiotics or immunosuppressive medication during the two months preceding enrolment. Other exclusion criteria were diabetes, inflammatory bowel disease, known liver disease of any other aetiology, and clinically important cardiovascular, pulmonary or renal co-morbidities. Patients with alcoholic hepatitis were enrolled from the InTeam Consortium (ClinicalTrials.gov identifier number: NCT02075918) from centres in the USA, Mexico, UK, France and Spain. Inclusion criteria for this study were active alcohol abuse (>50 g/day for men and >40 g/day for women) in the past 3 months, aspartate aminotransferase (AST) > ALT and total bilirubin >3 mg/dl in the past 3 months, and a liver biopsy and/or clinical picture consistent with alcoholic hepatitis. Exclusion criteria were autoimmune liver disease (ANA >1/320), chronic viral hepatitis, hepatocellular carcinoma, complete portal vein thrombosis, extrahepatic terminal disease, pregnancy and a lack of signed informed consent. In all patients, the clinical picture was consistent with alcoholic hepatitis and in patients who underwent liver biopsy, the histology was consistent with the diagnosis of alcoholic hepatitis. Liver biopsies were only done if clinically indicated as part of routine clinical care for diagnostic purposes of alcoholic hepatitis. Bio-specimens were collected during their admission to the hospital. The median time of specimen collection was 4 days following admission to the hospital (range 0–24, $n = 82$). For one patient who underwent liver transplantation, the transplantation date was considered as date of death. Patients were censored at the time point at which they were last seen alive. The baseline characteristics are shown in Supplementary Tables 1, 2. Faecal 16S rRNA sequencing, *Enterococcus* culture and qPCR were performed. The MELD score, ABIC score and discriminant function were calculated from all alcoholic hepatitis patients from whom respective laboratory values were available. The protocol was approved by the Ethics Committee of Hôpital Huriez, Universidad Autonoma de Nuevo Leon, Hospital Universitari Vall d'Hebron, King's College London, Yale University, University of North Carolina at Chapel Hill, Weill Cornell Medical College, Columbia University, University of Wisconsin, VA San Diego Healthcare System, University of California San Diego (UCSD) and Université Catholique de Louvain. Patients were enrolled after written informed consent was obtained from each patient.

Mice

C57BL/6 mice were purchased from Charles River and used in Fig. 2h and Extended Data Fig. 2. C57BL/6 germ-free mice were bred at UCSD and used in Figs. 2a–g, 3, 4, Extended Data Figs. 3, 7 and 9. Sublytic *Atp4a*^{S/S}

mice on a C57BL/6 background have previously been described^{11,34} and heterozygous mice were used for breeding; sublytic *Atp4a*^{S/S} littermate mice and their wild-type littermates were used in Extended Data Fig. 5.

Female and male mice (age of 9–12 weeks) were placed on a chronic-binge ethanol diet (NIAAA model) as previously described¹⁵. Mice were fed with Lieber–DeCarli diet and the caloric intake from ethanol was 0% on days 1–5 and 36% from day 6 until the end of the study period. At day 16, mice were gavaged with a single dose of ethanol (5 g/kg body weight) in the early morning and killed 9 h later. Pair-fed control mice received a diet with an isocaloric substitution of dextrose.

Stool samples from patients with alcoholic hepatitis (Fig. 1) were used for faecal transplantation in germ-free mice. Mice were gavaged with 100 µl of stool samples (1 g stool dissolved in 30 ml Luria–Bertani (LB) medium containing 15% glycerol under anaerobic conditions), starting at an age of 5–6 weeks and repeated 2 weeks later. Two weeks after the second gavage, mice were placed on the ethanol or control (isocaloric) diet.

In studies of the effects of cytolysin, 5×10^8 CFUs of a cytolytic *E. faecalis* strain (FA2-2(pAM714)), a non-cytolytic *E. faecalis* strain (FA2-2(pAM771))⁵ (*E. faecalis* Δcytolysin) (kindly provided by M. S. Gilmore), or PBS (vehicle control) were fed to mice by gavage every third day, starting from day 6 through day 15 of ethanol feeding. Administration every third day was necessary, given that *E. faecalis* does not colonize mice¹¹ (Extended Data Fig. 2o). To determine the effect of phage treatment, 10^{10} PFUs of *E. faecalis* phages (or *C. crescentus* phage phiCbK as control)³⁵ were gavaged to the mice 1 day before the ethanol binge (at day 16). All animal studies were reviewed and approved by the Institutional Animal Care and Use Committee of UCSD.

Bacteriophage isolation and amplification

The *E. faecalis* strain from *Atp4a*^{S/S} mice faeces has previously been isolated¹¹ and was used to isolate phages Efmus1, Efmus2, Efmus3 and Efmus4 (phages specific to the *E. faecalis* strain isolated from mouse faeces were named as Efmus with a number (Ef for *E. faecalis*, mus for mouse, digit for isolation order). *E. faecalis* strains from human stool samples were isolated using methods described below, and the corresponding phages were named as Ef with patient number plus a digit (Ef for *E. faecalis*, last digit for isolation order). All *E. faecalis* strains were grown statically in brain–heart infusion (BHI) broth or on BHI agar at 37 °C. *C. crescentus* phage phiCbK was purified as previously described³⁵.

E. faecalis phages were isolated from untreated raw sewage water obtained from North City Water Reclamation Plant in San Diego. Fifty millilitres of raw sewage water was centrifuged at 8,000g for 1 min at room temperature to pellet large particles. The supernatant was passed through a 0.45-µm and then a 0.2-µm syringe filter (Whatman, PES membrane). One hundred microlitres of the clarified sewage was mixed with 100 µl overnight *E. faecalis* culture and then added to BHI broth top agar (0.5% agar) and poured over a BHI plate (1.5% agar). After overnight growth at 37 °C, the resulting plaques were recovered using a sterile pipette tip in 500 µl PBS. Phages were replaques on *E. faecalis* three more times to ensure that the phages were clonal isolates.

High-titre phage stocks were propagated by infecting 200 ml of exponentially growing *E. faecalis* at a multiplicity of infection of 0.1 in BHI broth containing 10 mM MgSO₄. Lysis was allowed to proceed for up to six hours at 37 °C with shaking. The lysates were centrifuged at 10,000g for 20 min at room temperature to remove the remaining bacterial cells and debris. Supernatant was then vacuum-filtered through a 0.2-µm membrane filter and kept at 4 °C until use.

Before mice were gavaged, 10–20 ml lysates were concentrated using Corning Spin-X UF Concentrators with 100,000-molecular weight cutoff (MWCO) to a volume of approximately 1 ml. Following concentration, the culture medium was replaced with PBS via diafiltration. The resulting lysate was further concentrated to a final volume of 0.5 ml and adjusted to the required PFUs.

Whole-genome sequencing for phages

For all phages except Efmus4, 10 ml of lysates were treated with 10 µg/ml each of DNase and RNase at 37 °C for 1 h and phages were precipitated by adding 1M NaCl and 10% (w/v) polyethylene glycol 8000 (PEG 8000) and incubated at 4 °C overnight. Precipitated phages were then pelleted by centrifugation at 10,000g for 10 min at 4 °C and resuspended in 500 µl of resuspension buffer (5 mM MgSO₄). Phage DNA was then extracted using Promega Wizard DNA Clean-up kit (Promega). Phage genomes were sequenced using a combination of Illumina and Oxford Nanopore Technologies (ONT) MinION platforms. Illumina sequencing libraries were prepared using the Nextera XT library kit with bead-based size selection before loading onto Illumina flow cells. Sequencing was performed with either Illumina MiSeq Reagent Kit v3 in 2 × 300-bp or NextSeq 500 Mid Output Kit in 2 × 150-bp paired-end formats. ONT MinION sequencing libraries were prepared using the Rapid Barcoding Kit (SQK-RBK004) and loaded onto MinION R9.4 flow cells. ONT reads were basecalled with Albacore v.2.3.4 (ONT). The sequence reads were demultiplexed and adapters trimmed from ONT reads using Porechop v.0.2.3³⁶. A hybrid Illumina-ONT de novo assembly was performed using the Unicycler v.0.4.7 pipeline³⁷. Subsequently, Pilon v.1.22³⁸ was used iteratively to polish the assemblies with Illumina reads until no additional corrections could be made.

For phage Efmus4, 10⁹ PFUs of the phage was filtered sequentially using 0.45-µm and 0.2-µm filters (VWR) and purified on a caesium chloride (CsCl) density gradient³⁹. One millilitre of the CsCl fraction was purified on Amicon YM-100 protein columns (Millipore) and treated with DNase I. DNA was isolated using a Qiagen UltraSens virus kit (Qiagen), amplified using GenomiPhi V2 (GE Healthcare), and fragmented to 200 to 400 bp using a Bioruptor (Diagenode). Libraries were created using the Ion Plus fragment library kit and sequenced using a 316 Chip on an Ion Torrent Personal Genome Machine (Life Technologies). Reads were trimmed according to modified Phred scores of 0.5 using CLC Genomics Workbench 4.9 (Cambridge), and the remaining reads were assembled using CLC Genomics Workbench 4.9 based on 98% identity with a minimum of 50% read overlap³⁹. Reads were assembled into a single contig of 18,186 bp (20,118 × coverage).

Mapping of ONT reads to the hybrid assemblies was used to determine the orientation and terminal ends of linear phage genomes, and reference genomes served as guides to orient circular phage genomes. Phage genome assemblies were annotated using the NCBI Prokaryotic Genome Annotation Pipeline (PGAP)^{40,41}.

Phage raw sequence reads and annotated genomes are available at NCBI under the following consecutive BioSample IDs (SAMN11089809–SAMN11089827). GenBank accession numbers include: Efmus1 (MK721195), Efmus2 (MK721197), Efmus3 (MK721185), Efmus4 (MK721193), Ef2.1 (MK693030), Ef2.2 (MK721189), Ef2.3 (MK721192), Ef5.1 (MK721199), Ef5.2 (MK721186), Ef5.3 (MK721200), Ef5.4 (MK721191), Ef6.1 (MK721187), Ef6.2 (MK721188), Ef6.3 (MK721196), Ef6.4 (MK721190), Ef7.1 (MK721194), Ef7.2 (MK721183), Ef7.3 (MK721184) and Ef7.4 (MK721198).

Genetic maps of phage genomes were generated by LinearDisplay.pl (<https://github.com/JCVenterInstitute/LinearDisplay>), a PERL script that uses Xfig (<https://sourceforge.net/projects/mcjl/>) to render high-quality images. Preliminary annotation of genes was derived from the automated annotation and from Phage_Finder⁴², which uses curated hidden Markov models and databases of core phage gene to annotate core gene functions. Annotation was then manually reviewed to assign the final colours.

Phage phylogenetic tree

A phage whole-genome phylogeny tree was generated from a pairwise distance matrix calculated with the MASH program, which approximates average nucleotide identity (ANI)⁴³. First, a sketch file was created from all the 19 *E. faecalis* phage genomes isolated and sequenced in

this study plus 54 *Enterococcus* phage genomes obtained from GenBank, with 5,000 12-mers generated per genome (mash sketch -k 12 -s 5000). The sketch file was then compared to all the initial phage genome sequences to generate the ANI matrix using the mash distance command using default settings. The GGRaSP R package was used to calculate the UPMGA phylogeny from the ANI distance matrix, after redundant phage genomes (genomes ANI >99.985) were removed using the GGRaSP R package with a user defined cutoff of 0.015 (ggrasp.cluster (threshold = 0.015)). The resulting dendrogram was translated into newick format using the APE R package⁴⁴, loaded into the iTOL tree viewer⁴⁵, and annotated with taxonomic information and manually entered clade identification.

Electron microscopy

Phage morphology was examined by transmission electron microscopy of negatively stained grids, prepared using the valentine method⁴⁶ with either 2% uranyl-acetate or 2% phosphotungstic acid, and examined at an acceleration voltage of 100 kV in the JEOL 1200 EX transmission electron microscope.

Bacterial DNA extraction and 16S rRNA sequencing

DNA from human stool samples, mouse liver sections or bacterial culture was extracted as previously described¹¹, and DNA from mouse faeces was extracted using QIAamp Fast DNA Stool kit (Qiagen). 16S rRNA PCR was completed using Illumina adaptor and barcode-ligated 16S primers targeting the V4 region of the 16S rRNA gene^{47,48}. Amplicons were purified using the Qiaquick PCR purification kit (Qiagen) using manufacturer's specifications. Purified amplicons were then quantified via TECAN assay (Tecan), normalized and pooled in preparation for 16S rRNA sequencing. Pooled library was quantified and checked for quality using Agilent 2100 Bioanalyzer (Agilent Technologies). Library was sequenced on Illumina MiSeq (Illumina) using V2 reagent chemistry, 500 cycles, 2 × 250-bp format using manufacturer's specifications. 16S sequence reads were processed and operational taxonomic units were determined using our MOTHUR-based 16S rDNA analysis workflow as previously described^{11,49}. Raw 16S sequence reads can be found in the NCBI Sequence Read Archive (SRA) associated with Bioproject PRJNA525701.

Real-time qPCR

Bacterial genomic DNA was extracted from human stool samples and mouse liver¹¹. RNA was extracted from mouse liver and cDNAs were generated¹¹. Primer sequences for mouse genes were obtained from the NIH qPrimerDepot. Primer sequences for *E. faecalis* 16S rRNA gene, *E. faecalis* *cylL*₅ and *cylL*₁ genes have previously been described^{50,51}. All primers used in this study are listed in Supplementary Table 9. Mouse gene expression and amplification of bacterial genes were determined with Sybr Green (Bio-Rad Laboratories) using ABI StepOnePlus real-time PCR system. The qPCR value of mouse genes was normalized to 18S.

E. faecalis isolation and whole-genome sequencing

To isolate *E. faecalis* strains from human subjects, 50–300 mg of human stool was resuspended in 500 µl PBS, serial dilutions were made and 100 µl was placed on plates with selective medium, BBL Enterococcosel broth (Becton Dickinson). *Enterococci* colonies were identified by the production of dark brown or black colour, generated by hydrolysis of esculin to esculetin (which reacts with ferric ammonium citrate). Each *Enterococcus* colony was then picked, and qPCR was performed to identify *E. faecalis*, using specific primers against the *E. faecalis* 16S rRNA gene⁵⁰. For each subject, between 1 and 6 *E. faecalis* colonies were analysed and bacterial genomic DNA was then extracted as described in 'Bacterial DNA extraction and 16S rRNA sequencing'.

DNA sequencing was performed on the Illumina HiSeq Ten X generating paired-end reads (2 × 151 bp). Bacterial genomes were assembled

Article

and annotated using the previously described pipeline⁵². Antimicrobial resistance and virulence genes including cytolysin (*cyl*) genes carried by *E. faecalis* isolates were identified by comparing individual genome assemblies against the CARD and VFDB databases, respectively, using abricate v0.8.10 (<https://github.com/tseemann/abricate>)^{53,54}.

For the phylogeny of *E. faecalis*, the genome assemblies of the study isolates were annotated with Prokka⁵⁵, and a pangenome estimated using Roary⁵². A 95% identity cutoff was used, and core genes were defined as those in 99% of isolates. A maximum likelihood tree of the SNPs in the core genes was created using RAxML⁵⁶ and 100 bootstraps. The resulting tree was visualized using iTOL⁴⁵. Genome sequence data of *E. faecalis* strains isolated in this study have been deposited in the European Nucleotide Archive (ENA) under the accession number PRJEB25007. Sequence reads are available at ENA under run accession identifiers ERR3200171–ERR3200263.

E. faecalis culture

All *E. faecalis* strains were grown statically in BHI broth or on BHI agar plate at 37 °C. Fifty micrograms per millilitre erythromycin was added when cytolytic and non-cytolytic *E. faecalis* strains were grown (Extended Data Fig. 2).

Determination of levels of faecal *Enterococcus*

To determine levels of faecal enterococci in mice, 10–30 mg of mouse faeces was resuspended into 500 µl PBS and serial dilutions were made. Five microlitres of each dilution from each sample was spotted onto a plate with a selective medium, BBL enterococcosel broth (Becton Dickinson) and the plates were then incubated at 37 °C overnight. For Extended Data Fig. 2o, agar plates contained 50 µg/ml erythromycin. Enterococci colonies were identified by the production of a dark brown or black colour. Colony numbers of each sample were then counted, and CFUs were calculated.

Cytolysin expression and purification

To purify bioactive CylL_L'' and CylL_S'' , an *Escherichia coli* heterologous expression system was used. In brief, either 6×His–CylL_L or 6×His–CylL_S were co-expressed with CylM (the enzyme that performs dehydration and cyclization reactions on cytolysin) in *E. coli* to yield fully dehydrated and cyclized full-length peptides. The His tag and leader peptide were then removed using recombinant CylA (27–412), the soluble domain of the native peptidase used in cytolysin maturation, to yield bioactive CylL_L'' or CylL_S'' . The resulting core peptides were further purified by reversed-phase high-performance liquid chromatography (HPLC).

The *cylL_L* and *cylL_S* genes were previously cloned into the MCS1 of a pRSFDuet-1 backbone vector that contained the *cylM* gene in MCSII⁶. The *cylA* (27–412) gene was previously cloned into MCS1 of a pRSFDuet-1 backbone vector⁵⁷. *E. coli* BL21 Star (DE3) cells (50 µl) were transformed with 100 ng of either the *cylL_L:cylM*:pRSFDuet, *cylL_S:cylM*:pRSFDuet or *cylA* (27–412):pRSFDuet plasmids via KCM chemical transformation. The cells were plated on LB agar plates supplemented with kanamycin (50 µg/ml) and grown at 37 °C overnight. One colony was picked to inoculate 15 ml of LB broth supplemented with kanamycin overnight at 37 °C. The culture was used to inoculate 1.5 l of terrific broth supplemented with kanamycin. Cultures were grown with shaking at 37 °C to an optical density at 600 nm (OD₆₀₀) of 0.8. The temperature of the incubator was lowered to 18 °C and expression was induced with the addition of 0.3 mM final concentration of isopropyl β-D-thiogalactoside. The cultures were allowed to incubate at 18 °C for 18 h. The cells were collected by centrifugation at 5,000g for 12 min. The cell paste was collected and frozen at -70 °C.

For the purification of the protease CylA (27–412), the cell paste was thawed and resuspended in 50 ml LanP buffer (20 mM HEPES, 1 M NaCl, pH 7.5). The cell suspension was lysed by homogenization. The lysate was clarified by centrifugation at 13,000g for 45 min and filtered through a 0.45-µm centrifugal filter (Thermo Scientific). The clarified

lysate was applied to a pre-equilibrated HisTrap HP 5 ml column (GE Healthcare) through a peristaltic pump. The loaded column was connected to an ÄKTA pure 25 M system. The protein was eluted by a linear gradient of LanP buffer to Elution Buffer (20 mM HEPES, 1 M NaCl, 500 mM imidazole, 10% glycerol, pH 7.5) over 30 min. The purest fractions, as determined by 4–20% SDS–PAGE, were combined, concentrated to 1 mg/ml by Amicon Ultra Centrifugal Filters (30 kDa MWCO), and buffer exchanged into storage buffer (20 mM HEPES, 300 mM KCl, 10% glycerol, pH 7.5) by PD-10 desalting column (GE Healthcare). Protein concentration was determined by absorbance at 280 nm.

For the purification of CylL_L'' and CylL_S'' peptides, the cell paste was thawed and resuspended in 50 ml of LanA Buffer B1 (6 M guanidine HCl, 20 mM NaH₂PO₄, 500 mM NaCl, 0.5 mM imidazole, pH 7.5). The cell suspension was lysed via sonication (2-s pulse on, 5-s pulse off, 7 min total pulse on time). The cell lysate was clarified by centrifugation at 13,000g for 45 min. The clarified cell lysate was filtered through a 0.45-µm centrifugal filter and applied via gravity flow to a pre-equilibrated, 2 ml bed volume of His60 Ni Superflow Resin (Clonetech). After the lysate had been applied, the resin was washed with 15 ml of LanA Buffer B2 (4 M guanidine HCl, 20 mM NaH₂PO₄, 500 mM NaCl, 30 mM imidazole, pH 7.5). The resin was washed again with 15 ml of LanA Wash Buffer (20 mM NaH₂PO₄, 500 mM NaCl, 30 mM imidazole, pH 7.5) to remove the guanidine HCl. The peptides were eluted with 10 ml of LanA elution buffer (20 mM NaH₂PO₄, 500 mM NaCl, 500 mM imidazole, pH 7.5). A 0.02 mg/ml final concentration of CylA (27–412) was added to the elution fraction and allowed to incubate at room temperature overnight to remove the leader peptide.

The digestion was quenched by adding 2% (v/v) final concentration of trifluoroacetic acid. The solution was centrifuged at 4,500g for 10 min and filtered through a 0.45-µm syringe filter (Thermo Scientific). The core peptides were purified by semi-preparative reverse-phase HPLC using a Phenomenex Jupiter Proteo column (10 mm × 250 mm, 4 µm, 90 Å) connected to an Agilent 1260 Infinity II liquid chromatography system. The peptides were separated using a linear gradient of 3% (v/v) solvent B (acetonitrile + 0.1% trifluoroacetic acid) in solvent A (water + 0.1% trifluoroacetic acid). The fractions were spotted on a matrix-assisted laser desorption/ionization (MALDI) target plate by mixing 1 µl of sample with 1 µl of a 25 mg/ml solution of Super-DHB (Sigma) in 80% acetonitrile/water + 0.1% trifluoroacetic acid. The fractions were analysed by MALDI–time of flight (TOF) mass spectrometry on a Bruker UltrafleXtreme MALDI–TOF/TOF operating in positive ionization, reflector mode.

Primary mouse hepatocytes

Hepatocytes were isolated from C57BL/6 female mice fed the chronic-binge ethanol diet (NIAAA model)¹⁵. Livers were perfused in situ with 0.5 mM EGTA containing calcium-free salt solution and then perfused with a solution containing 0.02% (w/v) collagenase D (Roche Applied Science). Livers were then carefully minced and filtered using a 70-µm nylon cell strainer. Hepatocytes were centrifuged at 50g for 1 min after 3 washes. Hepatocyte viability was assessed by Trypan Blue (Thermo Fisher Scientific). Hepatocytes (1.5 × 10⁵) were seeded on 12-well plates coated with rat collagen type I in DMEM-F12 (Thermo Fisher Scientific) with insulin–transferrin–selenium (1% v/v) (Thermo Fisher Scientific) and 40 ng/ml dexamethasone (MP Biomedicals) containing 10% (v/v) fetal bovine serum (FBS) (Gemini Bio-Products) and antibiotics. After 4 h, the culture was washed with DMEM-F12 medium and changed to the same complemented medium without FBS⁵⁸. Then 16 h later, hepatocytes were cultured with 0 or 25 mM ethanol and stimulated with 0, 200 or 400 nM CylL_S'' and/or CylL_L'' in the same culture medium without FBS. After 3 h stimulation, hepatocyte cytotoxicity was assessed using Pierce LDH cytotoxicity detection kit (Thermo Fisher Scientific).

Biochemical analysis

Serum levels of ALT were determined using Infinity ALT kit (Thermo Scientific). Hepatic triglyceride levels were measured using Triglyceride

Liquid Reagents kit (Pointe Scientific). Levels of serum lipopolysaccharide and faecal albumin were determined by enzyme-linked immunosorbent kits (Lifeome Biolabs and Bethyl Labs, respectively). Serum levels of ethanol were measured using ethanol assay kit (BioVision).

Staining procedures

Formalin-fixed tissue samples were embedded in paraffin and stained with H & E. To determine lipid accumulation, liver sections were embedded in OCT compound. Eight-micrometre frozen sections were then cut and stained with Oil Red O (Sigma-Aldrich). Representative images from each group of mice are shown in each figure. The terminal deoxynucleotide transferase-mediated dUTP nick-end labelling (TUNEL) assay was performed using an in situ cell death detection kit (Sigma-Aldrich). We randomly selected five high-power fields for counting TUNEL-positive cells and normalized numbers to total cells.

Statistical analysis

Results are expressed as mean \pm s.e.m. (except when stated otherwise). Univariate and multivariate Cox regression analysis was used to detect associations of cytolysin with overall mortality. The multivariate model was adjusted for geographical origin of the patients, antibiotic treatment, platelet count, and creatinine, bilirubin and INR as components of the MELD score. Univariate logistic regression analysis of laboratory and clinical parameters associated with the detection of cytolysin and *E. faecalis* was performed. Univariate linear regression analysis of laboratory and clinical parameters associated with the log-transformed total amount of faecal *E. faecalis* measured with qPCR was performed. To associate log-transformed total *E. faecalis* and *E. faecalis* positivity with mortality, univariate Cox regression was used. *P* values from univariate and multivariate Cox regression, univariate logistic regression and univariate linear regression were determined by Wald test. Multicollinearity was examined using the variance inflation factor. Kaplan–Meier curves were used to compare survival between cytolysin-positive and cytolysin-negative patients with alcoholic hepatitis. Faecal *E. faecalis*, bacterial diversity and richness from controls and patients were compared using Kruskal–Wallis test with Dunn's post hoc test. Region- and/or centre-specific clinical characteristics of patients with alcoholic hepatitis were compared with Kruskal–Wallis test for continuous and Fisher's exact test for categorical variables. Faecal *E. faecalis* in patients with alcoholic hepatitis with or without cytolysin, and with or without cirrhosis, were compared with Mann–Whitney–Wilcoxon rank-sum test. Faecal *E. faecalis* in patients with alcoholic hepatitis from different region and/or centres were compared with the Kruskal–Wallis test. The percentage of subjects with faecal samples that were positive for *E. faecalis* and cytolysin was compared using Fisher's exact test, followed by FDR procedures for multiple group comparisons. Jaccard dissimilarity matrices were used for PCoA, and *P* values were determined by PERMANOVA followed by FDR procedures to correct for multiple comparisons.

For mouse and cell culture studies, the significance of multiple groups was evaluated using one-way or two-way ANOVA with Tukey's post hoc test. Fisher's exact test was used in the analysis of liver *E. faecalis* and cytolysin with FDR correction for multiple comparisons. Kaplan–Meier curves were used to compare survival between experimental mouse groups. PCoA based on Jaccard dissimilarity matrices was performed between experimental mouse groups and the *P* values were determined by PERMANOVA followed by FDR procedures to correct for multiple comparisons.

Exact *P* values for all comparisons, together with group size for each group, were listed in Supplementary Table 10. Statistical analyses were performed using R statistical software, R v.3.5.1 (R Foundation for Statistical Computing) and GraphPad Prism v.6.01. A value of *P* < 0.05 was considered to be statistically significant (adjusted for multiple comparisons when performing multiple tests).

Reporting summary

Further information on research design is available in the Nature Research Reporting Summary linked to this paper.

Data availability

Raw 16S sequence reads can be found in the NCBI SRA associated with Bioproject PRJNA525701. Phage raw sequence reads and annotated genomes are available at NCBI under the following consecutive BioSample identifiers (SAMN11089809–SAMN11089827). Genome sequence data of *E. faecalis* strains isolated in this study were registered at the ENA under study PRJEB25007.

Code availability

The PERL script for making the genetic maps of phage genomes can be found at <https://github.com/JCVenterInstitute/LinearDisplay>.

- Brandl, K. et al. Dysregulation of serum bile acids and FGF19 in alcoholic hepatitis. *J. Hepatol.* **69**, 396–405 (2018).
- Gao, B. et al. Serum and fecal oxylipins in patients with alcohol-related liver disease. *Dig. Dis. Sci.* **64**, 1878–1892 (2019).
- Lang, S. et al. Intestinal fungal dysbiosis and systemic immune response to fungi in patients with alcoholic hepatitis. *Hepatology* (2019).
- Ball, S. A., Tennen, H., Poling, J. C., Kranzler, H. R. & Rounsaville, B. J. Personality, temperament, and character dimensions and the DSM-IV personality disorders in substance abusers. *J. Abnorm. Psychol.* **106**, 545–553 (1997).
- Krieg, L. et al. Mutation of the gastric hydrogen-potassium ATPase alpha subunit causes iron-deficiency anemia in mice. *Blood* **118**, 6418–6425 (2011).
- Gill, J. J. et al. The *Caulobacter crescentus* phage phiCbk: genomics of a canonical phage. *BMC Genomics* **13**, 542 (2012).
- Wick, R. R., Judd, L. M., Gorrie, C. L. & Holt, K. E. Completing bacterial genome assemblies with multiplex MinION sequencing. *Microb. Genom.* **3**, e000132 (2017).
- Wick, R. R., Judd, L. M., Gorrie, C. L. & Holt, K. E. Unicycler: resolving bacterial genome assemblies from short and long sequencing reads. *PLOS Comput. Biol.* **13**, e1005595 (2017).
- Walker, B. J. et al. Pilon: an integrated tool for comprehensive microbial variant detection and genome assembly improvement. *PLoS ONE* **9**, e112963 (2014).
- Santiago-Rodriguez, T. M. et al. Transcriptome analysis of bacteriophage communities in periodontal health and disease. *BMC Genomics* **16**, 549 (2015).
- Haft, D. H. et al. RefSeq: an update on prokaryotic genome annotation and curation. *Nucleic Acids Res.* **46**, D851–D860 (2018).
- Tatusova, T. et al. NCBI prokaryotic genome annotation pipeline. *Nucleic Acids Res.* **44**, 6614–6624 (2016).
- Fouts, D. E. Phage_Finder: automated identification and classification of prophage regions in complete bacterial genome sequences. *Nucleic Acids Res.* **34**, 5839–5851 (2006).
- Ondov, B. D. et al. Mash: fast genome and metagenome distance estimation using MinHash. *Genome Biol.* **17**, 132 (2016).
- Paradis, E. & Schliep, K. ape 5.0: an environment for modern phylogenetics and evolutionary analyses in R. *Bioinformatics* **35**, 526–528 (2019).
- Letunic, I. & Bork, P. Interactive tree of life (iTOL) v3: an online tool for the display and annotation of phylogenetic and other trees. *Nucleic Acids Res.* **44**, W242–W245 (2016).
- Valentine, R. C., Shapiro, B. M. & Stadtman, E. R. Regulation of glutamine synthetase. XII. Electron microscopy of the enzyme from *Escherichia coli*. *Biochemistry* **7**, 2143–2152 (1968).
- Haas, B. J. et al. Chimeric 16S rRNA sequence formation and detection in Sanger and 454-pyrosequenced PCR amplicons. *Genome Res.* **21**, 494–504 (2011).
- Caporaso, J. G. et al. Global patterns of 16S rRNA diversity at a depth of millions of sequences per sample. *Proc. Natl Acad. Sci. USA* **108** (Suppl 1), 4516–4522 (2011).
- Chen, P. et al. Supplementation of saturated long-chain fatty acids maintains intestinal eubiosis and reduces ethanol-induced liver injury in mice. *Gastroenterology* **148**, 203–214.e16 (2015).
- Ryu, H. et al. Development of quantitative PCR assays targeting the 16S rRNA genes of *Enterococcus* spp. and their application to the identification of *enterococcus* species in environmental samples. *Appl. Environ. Microbiol.* **79**, 196–204 (2013).
- Haas, W., Shepard, B. D. & Gilmore, M. S. Two-component regulator of *Enterococcus faecalis* cytolysin responds to quorum-sensing autoinduction. *Nature* **415**, 84–87 (2002).
- Page, A. J. et al. Robust high-throughput prokaryote *de novo* assembly and improvement pipeline for Illumina data. *Microb. Genom.* **2**, e000083 (2016).
- Chen, L. et al. VFDB: a reference database for bacterial virulence factors. *Nucleic Acids Res.* **33**, D325–D328 (2005).
- Jia, B. et al. CARD 2017: expansion and model-centric curation of the comprehensive antibiotic resistance database. *Nucleic Acids Res.* **45**, D566–D573 (2017).
- Seemann, T. Prokka: rapid prokaryotic genome annotation. *Bioinformatics* **30**, 2068–2069 (2014).
- Stamatakis, A. RAxML version 8: a tool for phylogenetic analysis and post-analysis of large phylogenies. *Bioinformatics* **30**, 1312–1313 (2014).

Article

57. Tang, W., Bobeica, S. C., Wang, L. & van der Donk, W. A. CylA is a sequence-specific protease involved in toxin biosynthesis. *J. Ind. Microbiol. Biotechnol.* **46**, 537–549 (2019).
58. Iwaisako, K. et al. Protection from liver fibrosis by a peroxisome proliferator-activated receptor δ agonist. *Proc. Natl Acad. Sci. USA* **109**, E1369–E1376 (2012).
59. Clarke, T. H., Brinkac, L. M., Sutton, G. & Fouts, D. E. GGRaSP: a R-package for selecting representative genomes using Gaussian mixture models. *Bioinformatics* **34**, 3032–3034 (2018).

Acknowledgements S. Lang was supported by a DFG fellowship (LA 4286/1-1), C.L. was supported by an AASLD Pinnacle Research Award in Liver Disease and a pilot project award from Southern California Research Center for Alcoholic Liver and Pancreatic Disease (ALPD) and Cirrhosis (P50 AA011999), Y.S. was supported by a Wellcome Trust PhD studentship and I.R.R. was supported by National Institute of General Medical Sciences (NIGMS)–NIH Chemistry–Biology Interface Training Grant (T32-GM070421). This study was supported in part by a Biocodex Microbiota Foundation Grant, NIH grants R01 AA24726, U01 AA026939, by Award Number BX004594 from the Biomedical Laboratory Research & Development Service of the VA Office of Research and Development (to B.S.), the Wellcome Trust (WT098051) (to T.D.L.), NIH grant U01AA021908 (to R.B.) and services provided by P30 DK120515 and P50 AA011999.

Author contributions Y.D. was responsible for acquisition, analysis and interpretation of data, and drafting of the manuscript; C.L. was responsible for study concept and design, acquisition,

analysis and interpretation of data and key preliminary experiments; S. Lang, K.B., J.L. and X.M.T. provided assistance with statistical analysis; H.C., L.J., B.G., W.S., R.K., F.H. and S. Lee provided assistance with data acquisition; R.C.W., T.H.C., K.N., M.T. and D.E.F. were responsible for 16S rRNA sequencing, phage genome sequencing and data analysis; Y.S. and T.D.L. were responsible for bacterial genome sequencing and data analysis; A.H.-M., L.L. and R.Y. provided assistance with phage studies and were responsible for electron microscopy data; R.Y. provided critical revision of the manuscript; I.R.R. and W.A.v.d.D. were responsible for cytolysin expression and purification; Y.M. and L.E. provided assistance with the design and conduct of the gnotobiotic mouse studies; M.L. and D.P. provided assistance with phage isolation; M.V.-C., F.B.-P., E.C.V., J.G.A., R.S.B. Jr, V.V., J.A., J.C., D.L.S., S.B.H., A.L., M.R.L., P.M., G.G.-T., R.B. and P.S. were responsible for collection of human samples; D.E.F. and B.S. were responsible for the study concept and design, and editing the manuscript; B.S. was responsible for study supervision.

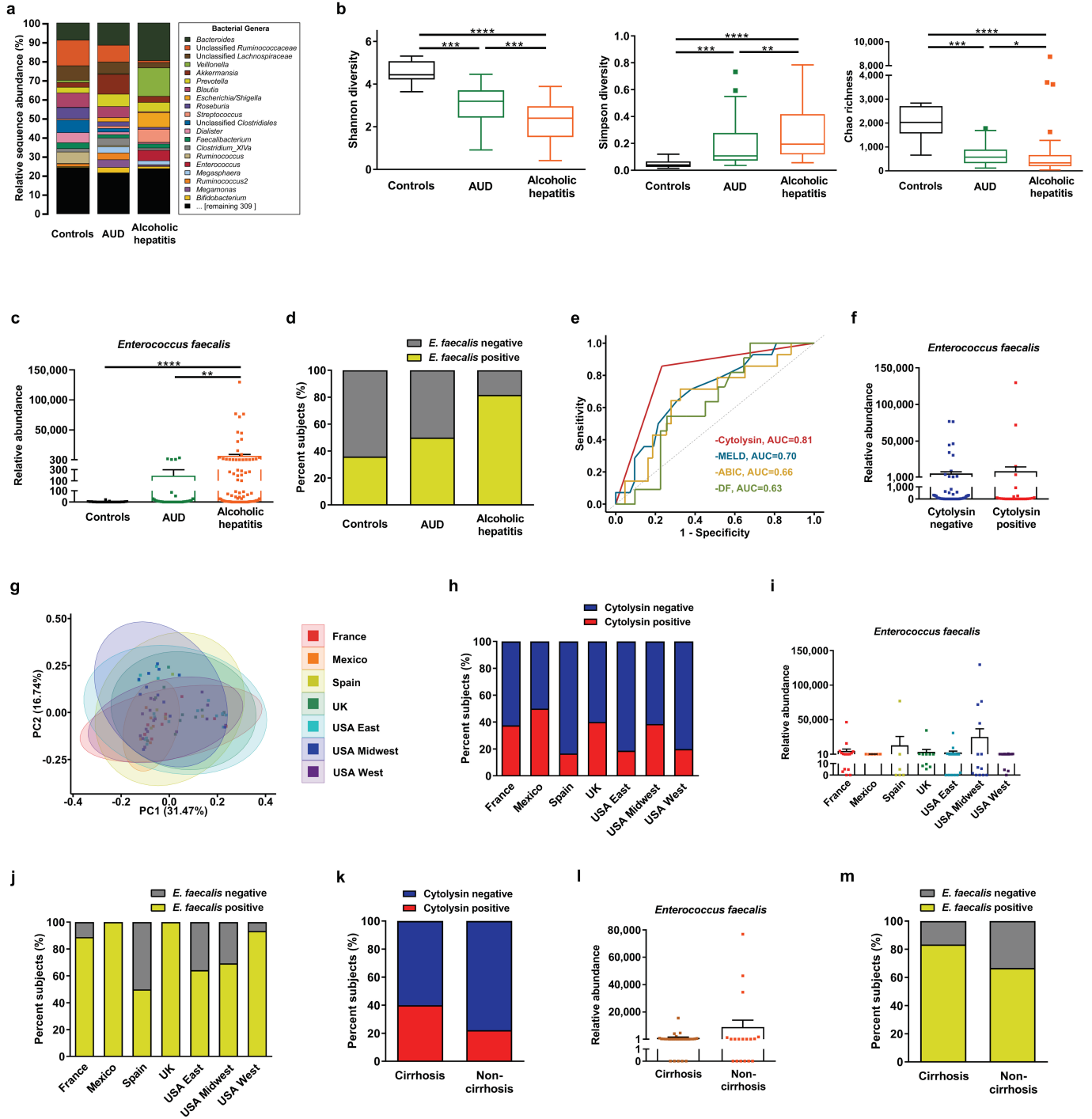
Competing interests B.S. consults for the Ferring Research Institute; however, there is no competing interest with regard to this study. All other authors declare no competing interests.

Additional information

Supplementary information is available for this paper at <https://doi.org/10.1038/s41586-019-1742-x>.

Correspondence and requests for materials should be addressed to B.S.

Reprints and permissions information is available at <http://www.nature.com/reprints>.

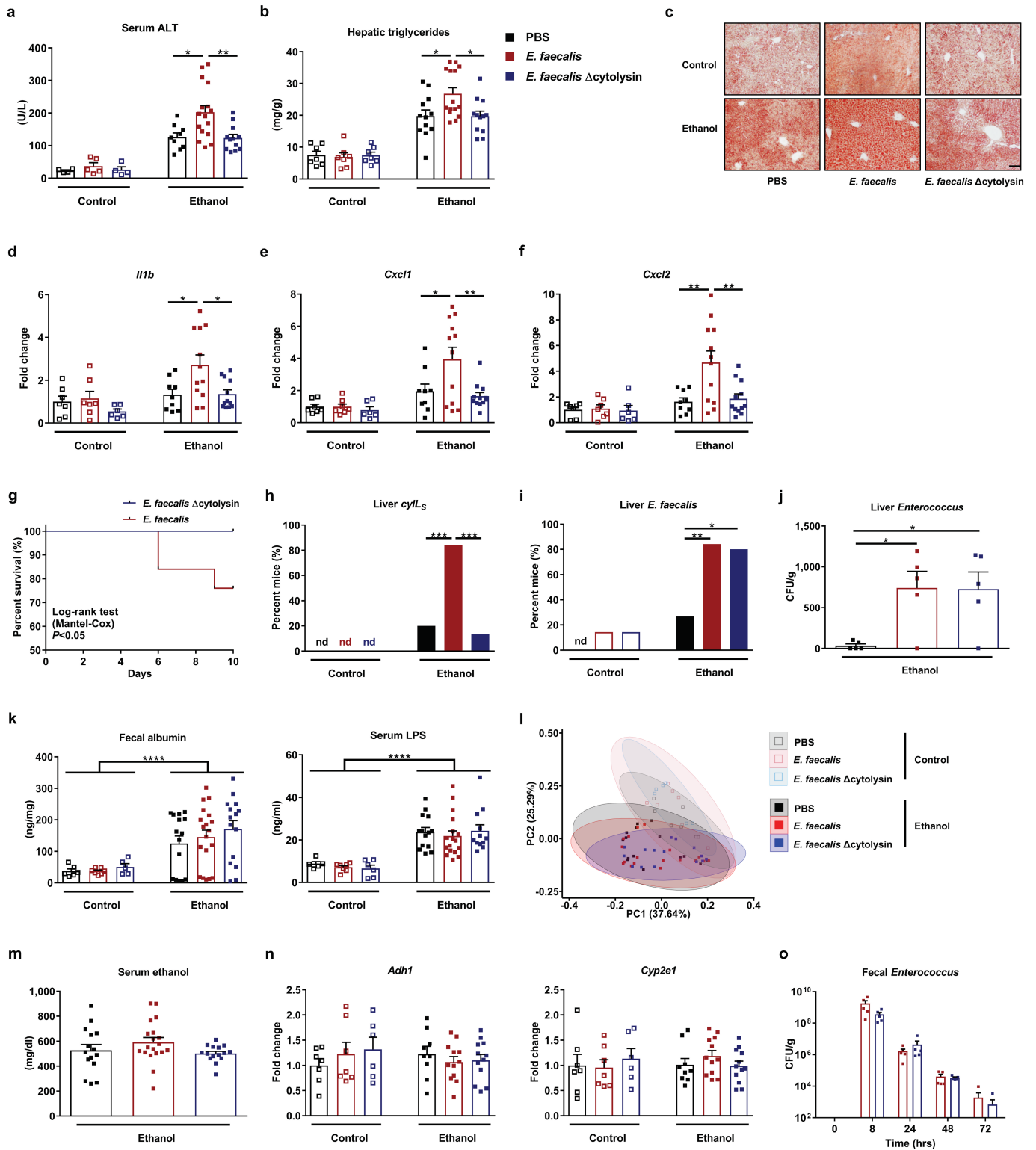


Extended Data Fig. 1 | See next page for caption.

Extended Data Fig. 1 | Intestinal dysbiosis in patients with alcoholic

hepatitis. a, 16S rRNA sequencing of faecal samples from controls ($n = 14$), patients with alcohol-use disorder ($n = 43$), or alcoholic hepatitis ($n = 75$). The graph demonstrates the relative abundance of sequence reads in each genus. **b**, Bacterial diversity (Shannon index and Simpson index) and richness (Chao richness) was calculated in controls ($n = 14$), patients with alcohol-use disorder ($n = 43$) or alcoholic hepatitis ($n = 75$). **c**, *E. faecalis* in faecal samples from controls ($n = 25$), patients with alcohol-use disorder ($n = 38$) or alcoholic hepatitis ($n = 82$), assessed by qPCR. **d**, Percentage of faecal samples positive for *E. faecalis* in controls ($n = 25$), patients with alcohol-use disorder ($n = 38$) or alcoholic hepatitis ($n = 82$), assessed by qPCR. *E. faecalis* was detected in faeces from 80% of patients with alcoholic hepatitis, versus 36% of controls ($P < 0.001$). There was also a significant difference between patients with alcohol-use disorder and patients with alcoholic hepatitis ($P < 0.01$). **e**, Receiver operating characteristic curves and area under the curve (AUC) for the comparison of 90-day mortality and cytolysin positivity (red; $n = 57$), MELD score (blue; $n = 56$), ABIC score (yellow; $n = 57$) and discriminant function (green; $n = 42$) in patients with alcoholic hepatitis. **f**, *E. faecalis* in faecal samples from patients with alcoholic hepatitis whose faecal samples were cytolysin-positive ($n = 25$) or cytolysin-negative ($n = 54$), assessed by qPCR ($P = 0.8174$). **g**, 16S rRNA sequencing of faecal samples from patients with alcoholic hepatitis from different centres (France, $n = 9$; Mexico, $n = 6$; Spain, $n = 5$; UK, $n = 11$; USA (east), $n = 16$; USA (Midwest), $n = 12$; USA (west), $n = 16$ patients). We used PCoA based on Jaccard dissimilarity matrices to show β -diversity among groups at the genus level. The composition of faecal microbiota was significantly different between patients from different regions ($P < 0.01$). **h**, Percentage of faecal samples that were positive for *cylL₁* and *cylL₅* DNA sequences (cytolysin-positive), in patients with alcoholic hepatitis from different centres (France,

$n = 16$; Mexico, $n = 6$; Spain, $n = 6$; UK, $n = 10$; USA (east), $n = 16$; USA (Midwest), $n = 13$; USA (west), $n = 15$ patients), assessed by qPCR ($P = 0.6094$). **i**, *E. faecalis* in faecal samples from patients with alcoholic hepatitis from different centres, assessed by qPCR ($P = 0.5648$). **j**, Percentage of faecal samples that were positive for *E. faecalis* in patients with alcoholic hepatitis from different centres (France, $n = 16$; Mexico, $n = 6$; Spain, $n = 6$; UK, $n = 10$; USA (east), $n = 16$; USA (Midwest), $n = 13$; USA (west), $n = 15$ patients), assessed by qPCR ($P = 0.0529$). **k**, Percentage of subjects with faecal samples that were positive for *cylL₁* and *cylL₅* DNA sequences (cytolysin-positive), in patients with alcoholic hepatitis and with ($n = 30$) or without ($n = 18$) cirrhosis, assessed by qPCR ($P = 0.3431$). **l**, *E. faecalis* in faecal samples from patients with alcoholic hepatitis and with ($n = 30$) or without ($n = 18$) cirrhosis, assessed by qPCR ($P = 0.5736$). **m**, Percentage of faecal samples that were positive for *E. faecalis* in patients with alcoholic hepatitis and with ($n = 30$) or without ($n = 18$) cirrhosis, assessed by qPCR ($P = 0.2878$). Results are expressed as mean \pm s.e.m. **(c, f, i, l)**. For the box and whisker plots in **b**, the box extends from the 25th to 75th percentiles, and the centre line represents the median; for all three groups, the bottom whiskers show the minimum values; for the control group (black), the top whisker shows the maximum value; for the other two groups, the top whiskers represent the 75th percentile plus 1.5 \times the inter-quartile distance (the distance between the 25th and 75th percentiles); all values greater than this are plotted as individual dots. *P* values were determined by Kruskal–Wallis test (**i**) with Dunn's post hoc test (**b, c**), two-sided Fisher's exact test (**h, j, k, m**) followed by FDR procedures (**d**), two-sided Mann–Whitney Wilcoxon rank-sum test (**f, l**) or PERMANOVA (**g**). The exact group size (n) and *P* values for each comparison are listed in Supplementary Table 10. * $P < 0.05$, ** $P < 0.01$, *** $P < 0.001$, **** $P < 0.0001$.

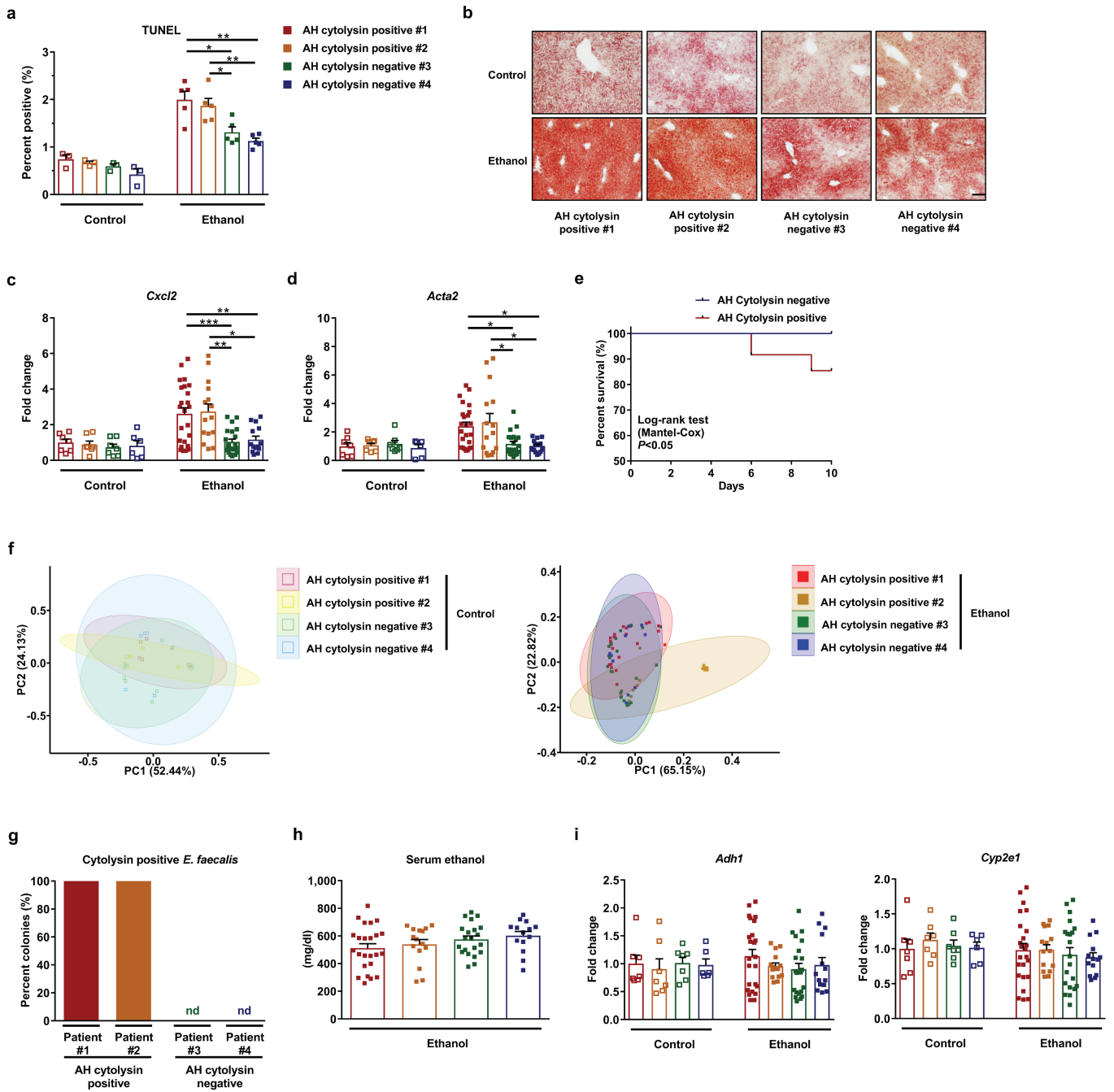


Extended Data Fig. 2 | See next page for caption.

Article

Extended Data Fig. 2 | Cytolytic *E. faecalis* causes the progression of ethanol-induced liver disease in mice. **a–n**, C57BL/6 mice were fed oral isocaloric (control) or chronic–binge ethanol diets and gavaged with vehicle (PBS), a cytolytic *E. faecalis* strain (FA2-2(pAM714)) (denoted *E. faecalis*) (5×10^8 CFUs) or a non-cytolytic *E. faecalis* strain (FA2-2(pAM771))⁵ (denoted *E. faecalis* Δ cytolysin) (5×10^8 CFUs) every third day. **a**, Serum levels of ALT. **b**, Hepatic triglyceride content. **c**, Representative oil red O-stained liver sections. **d–f**, Hepatic levels of mRNAs. **g**, Kaplan–Meier curve of survival of mice on chronic–binge ethanol diets (day 0 denotes the start of ethanol feeding). Mice gavaged with PBS all survived, and are not included in the figure. A higher proportion of mice ($n = 15$) gavaged with non-cytolytic *E. faecalis* survived than did mice ($n = 25$) gavaged with cytolytic *E. faecalis*. **h**, Proportions of mice that were positive for cytolysin in the liver, measured by qPCR for *cytL₅* (the gene that encodes cytolysin subunit CytL₅’). **i**, Proportions of mice that were positive for *E. faecalis* in the liver, measured by qPCR. About 80% of mice colonized with cytolytic *E. faecalis*, as well as those colonized with non-cytolytic *E. faecalis*, were positive for *E. faecalis* in their livers. **j**, Liver CFUs of *Enterococcus* in mice on a chronic–binge ethanol diet. **k**, Paracellular intestinal permeability was evaluated by measuring faecal albumin content and serum levels of lipopolysaccharide (LPS) by enzyme-linked immunosorbent assays. **l**, Faecal samples were collected and 16S rRNA genes were sequenced. PCoA based on Jaccard dissimilarity matrices showed no significant differences among mice gavaged with PBS, cytolytic or non-cytolytic *E. faecalis* following

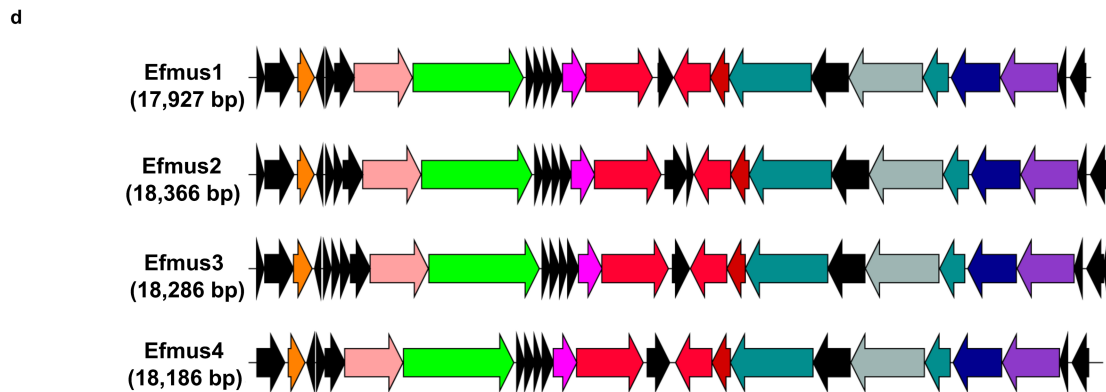
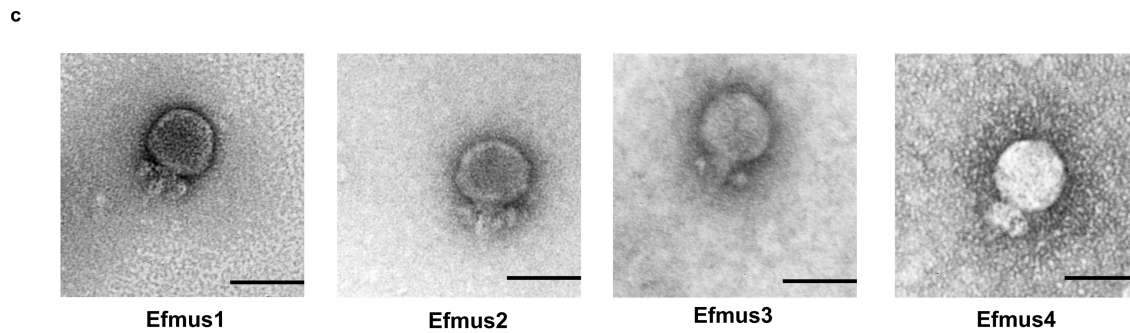
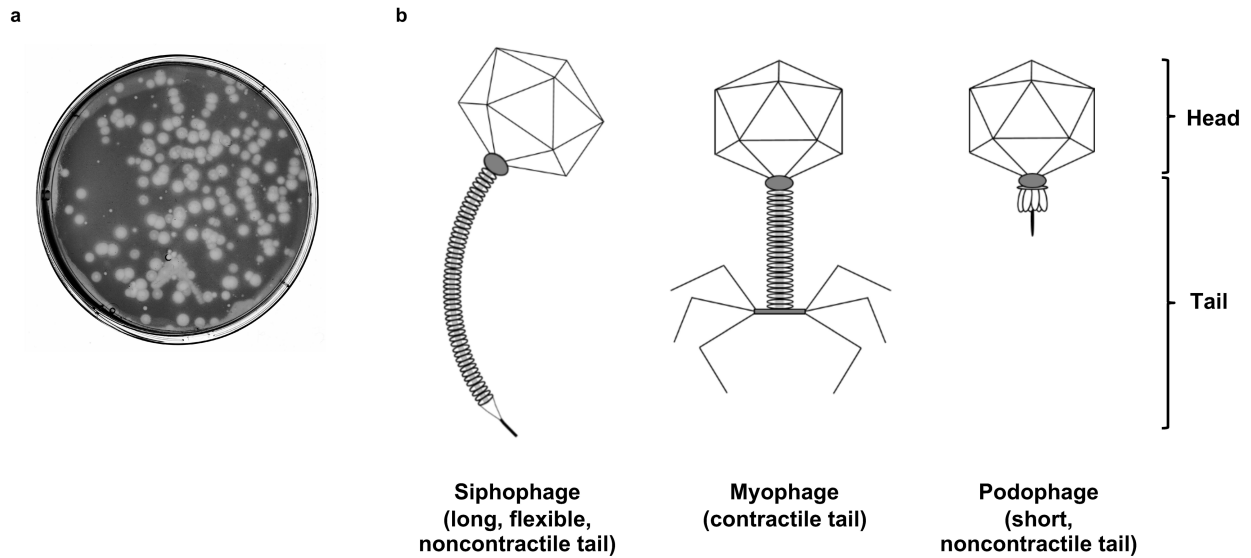
feeding with the control and ethanol diets. Compared to mice fed with a control diet, mice fed with an ethanol diet had significantly different faecal microbiomes after gavaging with *E. faecalis* ($P < 0.05$). **m, n**, Serum levels of ethanol and hepatic levels of *Adh1* and *Cyp2e1* mRNAs did not differ significantly among mice gavaged with PBS, cytolytic or non-cytolytic *E. faecalis* after ethanol feeding. **o**, Mice were gavaged with cytolytic or non-cytolytic *E. faecalis* strains (carrying the erythromycin resistance gene; 5×10^8 CFUs) at time 0, and faeces were collected 0, 8, 24, 48 and 72 h later. Faecal CFUs of *Enterococcus* were determined by culturing faecal samples on BBL enterococcosel broth agar plate with $50 \mu\text{g ml}^{-1}$ erythromycin. At time 0 and 72 h, five out of five and four out of five mice, respectively, had no detectable erythromycin-resistant *Enterococcus* in their faeces. These points are not shown on the graph, but have been included in the calculation of mean \pm s.e.m. Scale bar, $100 \mu\text{m}$. Results are expressed as mean \pm s.e.m. (**a, b, d–f, j, k, m–o**). *P* values among groups of mice fed with the control or ethanol diet were determined by one-way ANOVA with Tukey’s post hoc test (**a, b, d–f, j, k, m, n**), two-sided log-rank (Mantel–Cox) test (**g**), two-sided Fisher’s exact test followed by FDR procedures (**h, i**) or PERMANOVA followed by FDR procedures (**l**). All results were generated from at least three independent replicates. The exact group size (n) and *P* values for each comparison are listed in Supplementary Table 10. *P* values between mice fed with a control diet and mice fed with an ethanol diet were determined by two-way ANOVA (**k**). * $P < 0.05$, ** $P < 0.01$, *** $P < 0.001$, **** $P < 0.0001$.



Extended Data Fig. 3 | Transplantation of cytolyisin-positive faeces increases ethanol-induced liver disease in gnotobiotic mice.

a–f, h, i, C57BL/6 germ-free mice were colonized with faeces from two cytolyisin-positive and two cytolyisin-negative patients with alcoholic hepatitis, and then fed isocaloric (control) or chronic-binge ethanol diets. **a**, Percentage of TUNEL-positive hepatic cells. **b**, Representative oil red O-stained liver sections. **c, d**, Hepatic levels of mRNAs that encode the inflammatory cytokine *Cxcl2* and *Acta2* (a marker of activated hepatic stellate cells). **e**, Kaplan–Meier curve of survival of mice on chronic-binge ethanol diets (day 0 denotes the start of ethanol feeding), gavaged with faeces from cytolyisin-positive ($n = 48$ mice) or cytolyisin-negative ($n = 32$ mice) patients with alcoholic hepatitis. **f**, Faecal samples were collected and 16S rRNA genes were sequenced. The graph shows PCoA of faecal microbiomes. No significant difference was observed between mice colonized with faeces from cytolyisin-positive or cytolyisin-negative donors with alcoholic hepatitis, following the control diet. Mice transplanted with faeces from a cytolyisin-positive patient with alcoholic hepatitis (patient

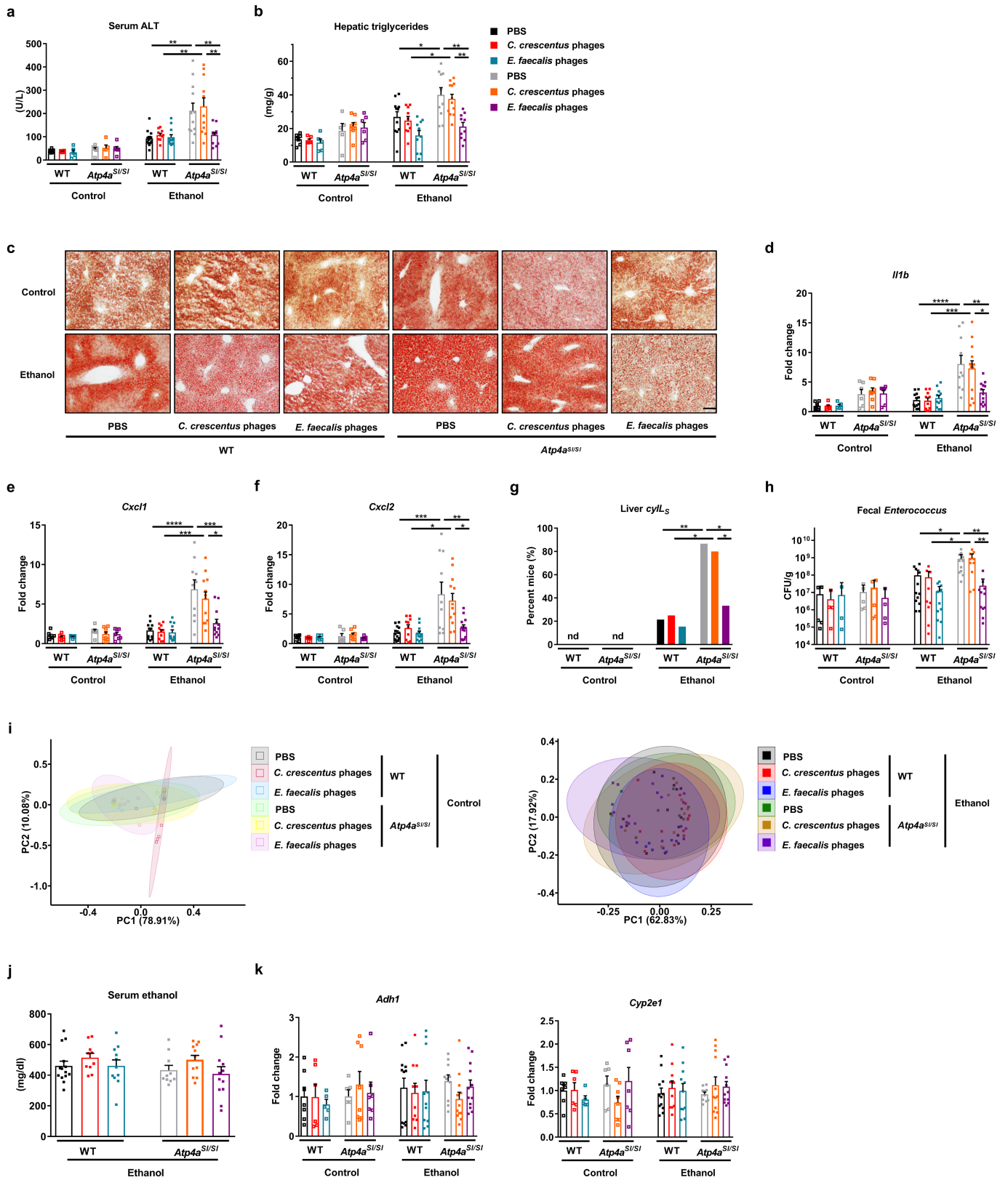
no. 2) showed a microbiota that was significantly different to that of the other mouse groups following ethanol administration ($P < 0.01$). **g**, Percentage of cytolyisin-positive *E. faecalis* in four patients with alcoholic hepatitis. Stool samples from the four patients were placed on plates with selective medium, and *Enterococcus* colonies were identified by the production of a dark brown or black colour. *Enterococcus* colonies were confirmed to be *E. faecalis* by qPCR. The cytolyisin status of each *E. faecalis* colony was determined by qPCR. **h**, Serum levels of ethanol were comparable among colonized mice after ethanol feeding. **i**, Hepatic levels of *Adh1* and *Cyp2e1* mRNAs did not differ significantly among colonized mice on control or ethanol diets. Scale bar, 100 μm. Results are expressed as mean \pm s.e.m. (**a, c, d, h, i**). P values were determined by one-way ANOVA with Tukey's post hoc test (**a, c, d, h, i**), two-sided log-rank (Mantel–Cox) test (**e**) or PERMANOVA followed by FDR procedures (**f**). All results were generated from at least three independent replicates. The exact group size (n) and P values for each comparison are listed in Supplementary Table 10. * $P < 0.05$, ** $P < 0.01$, *** $P < 0.001$.



Capsid structural components and assembly	Tail and baseplate assembly	DNA metabolism	Host cell lysis	Other
<p>encapsidation/terminase</p> <p>major capsid</p> <p>portal</p>	<p>tail fiber</p> <p>tail components</p>	<p>DNA polymerase</p> <p>DNA binding</p>	<p>endolysin/lysin</p> <p>holin</p>	<p>hypothetical protein</p> <p>intron/intein</p>

Extended Data Fig. 4 | Isolation and amplification of phages against cytolytic *E. faecalis* isolated from mice. **a**, BHI agar plate showing phage plaque morphology. The phage cocktail (100 μ l) (10^2 – 10^3 PFUs) was mixed with overnight-grown *E. faecalis* culture (100 μ l) and then added to BHI broth top agar (0.5% agar) and poured over a BHI plate (1.5% agar). After overnight growth at 37 $^{\circ}$ C, images were captured on an Epson Perfection 4990 Photo scanner. **b**, Simplified illustration of the morphologies of different phages. Siphophages have long, flexible noncontractile tails (left); myophages have contractile tails

(middle); and podophages have short noncontractile tails (right). **c**, Transmission electron microscopy revealed that phages we isolated were all podophages (Efmus1, Efmus2, Efmus3 and Efmus4). **d**, Genetic map of phage genomes. The linear maps are based on nucleotide sequences of the phage genomes and predicted open reading frames. The name and length (in bp) of each genome are indicated to the left of each phage map. Protein-coding sequences are coloured on the basis of functional role categories. Scale bar, 50 nm. All results were generated from at least three independent replicates.

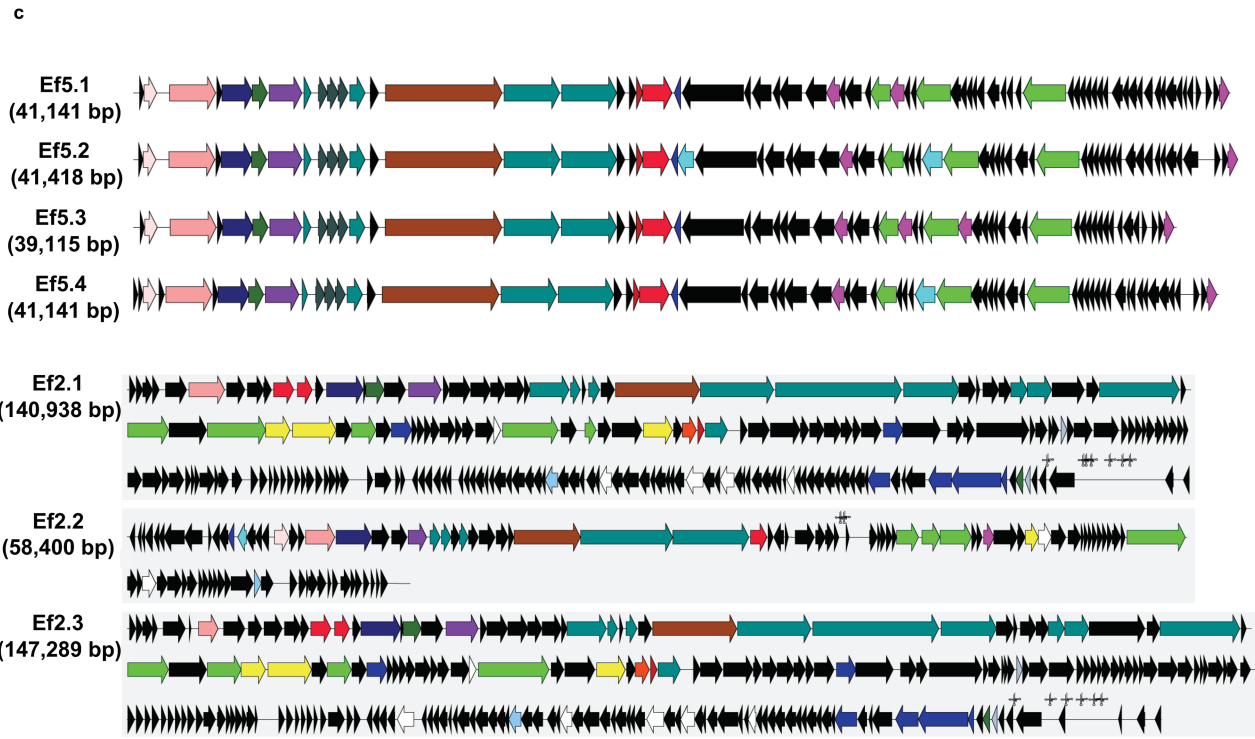
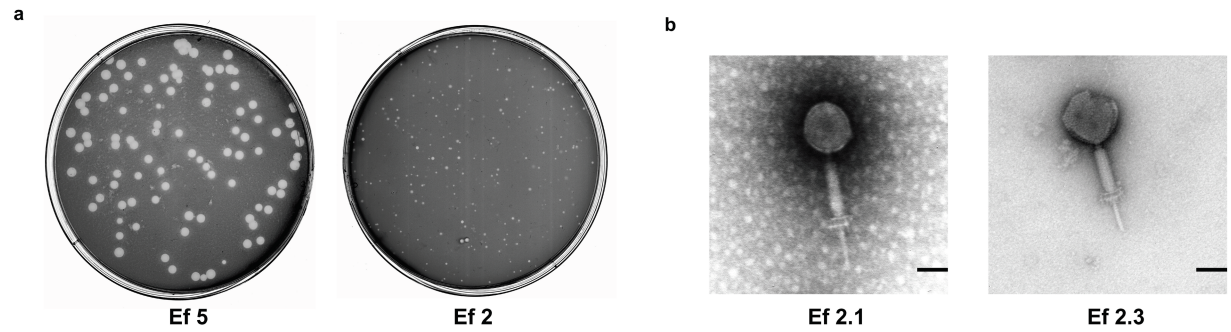


Extended Data Fig. 5 | See next page for caption.

Article

Extended Data Fig. 5 | Phages reduce translocation of cytolysin to the liver and reduce ethanol-induced liver disease in *Atp4a*^{Sl/Sl} mice. **a–k**, Wild-type (WT) and *Atp4a*^{Sl/Sl} littermates were fed oral isocaloric (control) or chronic-binge ethanol diets, and gavaged with vehicle (PBS), control phages against *C. crescentus* (10^{10} PFUs) or a cocktail of four different phages that target cytolysin *E. faecalis* (10^{10} PFUs), 1 day before an ethanol binge. **a**, Serum levels of ALT. **b**, Hepatic triglyceride content. **c**, Representative oil red O-stained liver sections. **d–f**, Hepatic levels of mRNAs. **g**, Proportions of mice that were positive for cytolysin in the liver, measured by qPCR for *cylL*₅. **h**, Faecal CFUs of *Enterococcus*. **i**, Faecal samples were collected and 16S rRNA genes were sequenced. PCoA based on Jaccard dissimilarity matrices found no significant

difference in faecal microbiota among mice given PBS, control phage or phages that target cytolysin *E. faecalis* in each group. **j, k**, Serum levels of ethanol and hepatic levels of *Adh1* and *Cyp2e1* mRNAs did not differ significantly among colonized mice after ethanol feeding. Scale bar, 100 μ m. Results are expressed as mean \pm s.e.m. (**a, b, d–f, h, j, k**). *P* values were determined by two-way ANOVA with Tukey's post hoc test (**a, b, d–f, h, j, k**), two-sided Fisher's exact test followed by FDR procedures (**g**) or PERMANOVA followed by FDR procedures (**i**). All results were generated from at least three independent replicates. The exact group size (*n*) and *P* values for each comparison are listed in Supplementary Table 10. **P* < 0.05, ***P* < 0.01, ****P* < 0.001, *****P* < 0.0001.

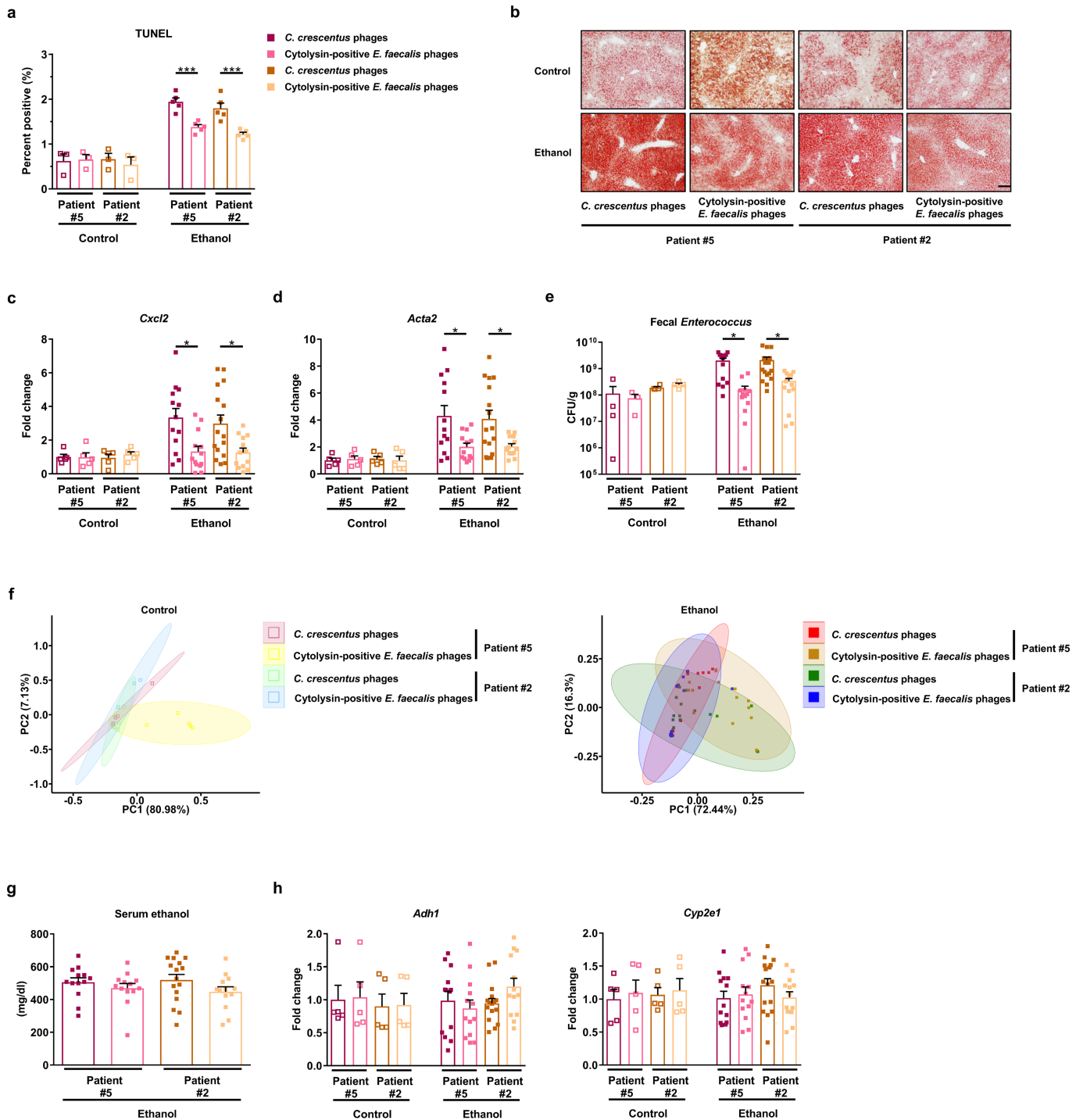


Capsid structural components and assembly	Tail and baseplate assembly	DNA metabolism	Host cell lysis	Other
<ul style="list-style-type: none"> encapsidation/terminase major capsid portal protease (scaffold protein) other 	<ul style="list-style-type: none"> tail fibers tail component tail measure 	<ul style="list-style-type: none"> DNA polymerase DNA binding DNA recombination salvage of nucleosides and nucleotides DNA restriction/modification nucleotide degradation 	<ul style="list-style-type: none"> endolysin/lysin holin 	<ul style="list-style-type: none"> hypothetical protein intron/intein regulatory transcription factor other known functions tRNA

Extended Data Fig. 6 | Isolation and amplification of phages against cytolytic *E. faecalis* strains isolated from patients with alcoholic hepatitis.

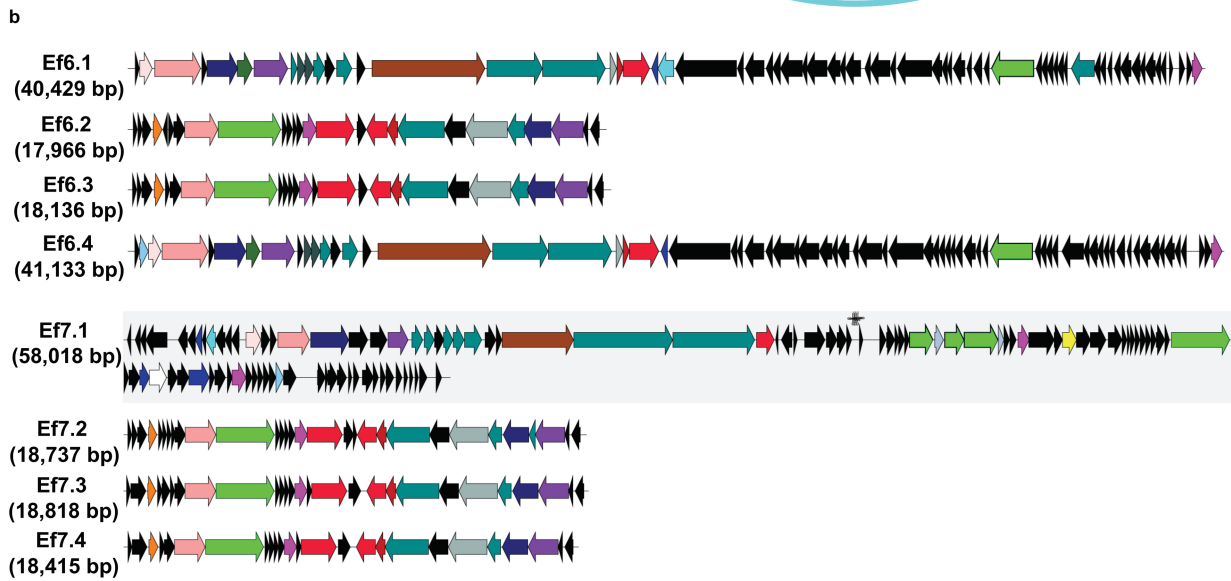
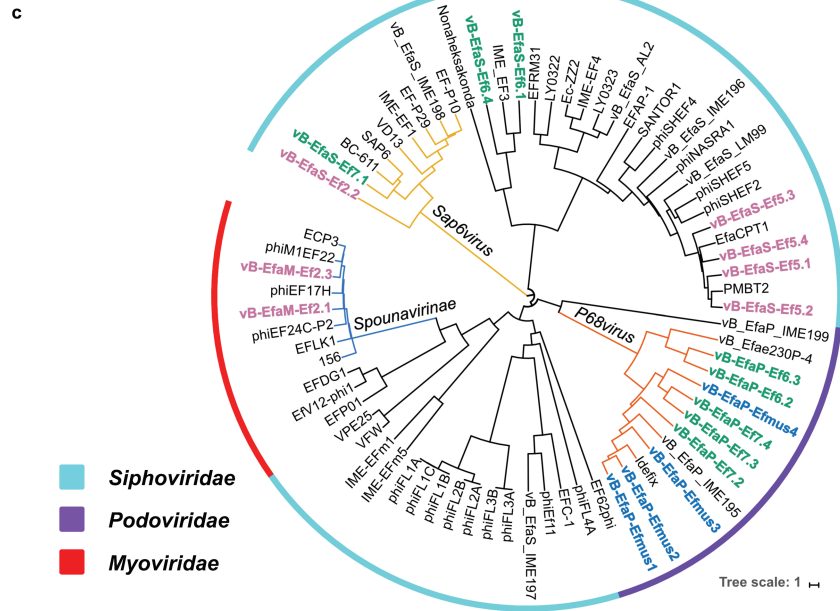
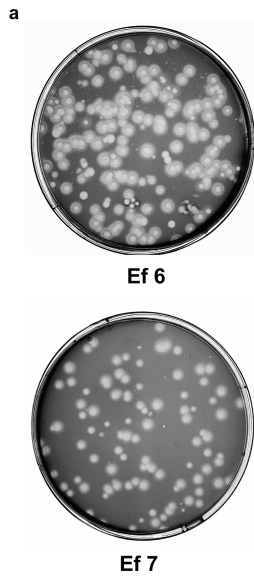
a, BHI agar plates showing phage plaque morphology. **b**, Transmission electron microscopy graphs of myophages Ef2.1 and Ef2.3, stained with phosphotungstic acid showing contracted tails. **c**, Genetic map of phage genomes. The linear maps are based on nucleotide sequences of the phage

genomes and predicted open reading frames. The name and length (in bp) of each genome are indicated to the left of each phage map. Protein-coding sequences are coloured on the basis of functional role categories. Sequences that encode tRNA genes are indicated by a cloverleaf structure. Scale bar, 50 nm. All results were generated from at least three independent replicates.



Extended Data Fig. 7 | Phages that target cytolytic *E. faecalis* reduce ethanol-induced liver disease in gnotobiotic mice. a–h, C57BL/6 germ-free mice were colonized with faeces from two cytolysin-positive patients with alcoholic hepatitis (faeces from one patient were also used in Fig. 2). The mice were then fed oral isocaloric (control) or chronic-binge ethanol diets, and gavaged with control phages against *C. crescentus* (10^{10} PFUs) or a cocktail of 3 or 4 different phages that target cytolytic *E. faecalis* (10^{10} PFUs), one day before an ethanol binge. **a**, Percentage of TUNEL-positive hepatic cells. **b**, Representative oil red O-stained liver sections. **c, d**, Hepatic levels of mRNAs that encode the inflammatory cytokine *Cxcl2*, and *Acta2* (a marker of activated hepatic stellate cells). **e**, Faecal CFUs of *Enterococcus*. **f**, Faecal samples were

collected and 16S rRNA genes were sequenced. PCoA based on Jaccard dissimilarity matrices shows no significant differences in the faecal microbiota of mice gavaged with control phage and phages that target cytolytic *E. faecalis* in each group. **g, h**, Serum levels of ethanol and hepatic levels of *Adh1* and *Cyp2e1* mRNAs did not differ significantly among colonized mice after ethanol feeding. Scale bar, 100 μ m. Results are expressed as mean \pm s.e.m. (**a, c–e, g, h**). *P* values were determined by two-way ANOVA with Tukey's post hoc test (**a, c–e, g, h**) or PERMANOVA followed by FDR procedures (**f**). All results were generated from at least three independent replicates. The exact group size (*n*) and *P* values for each comparison are listed in Supplementary Table 10. **P* < 0.05, ****P* < 0.001.



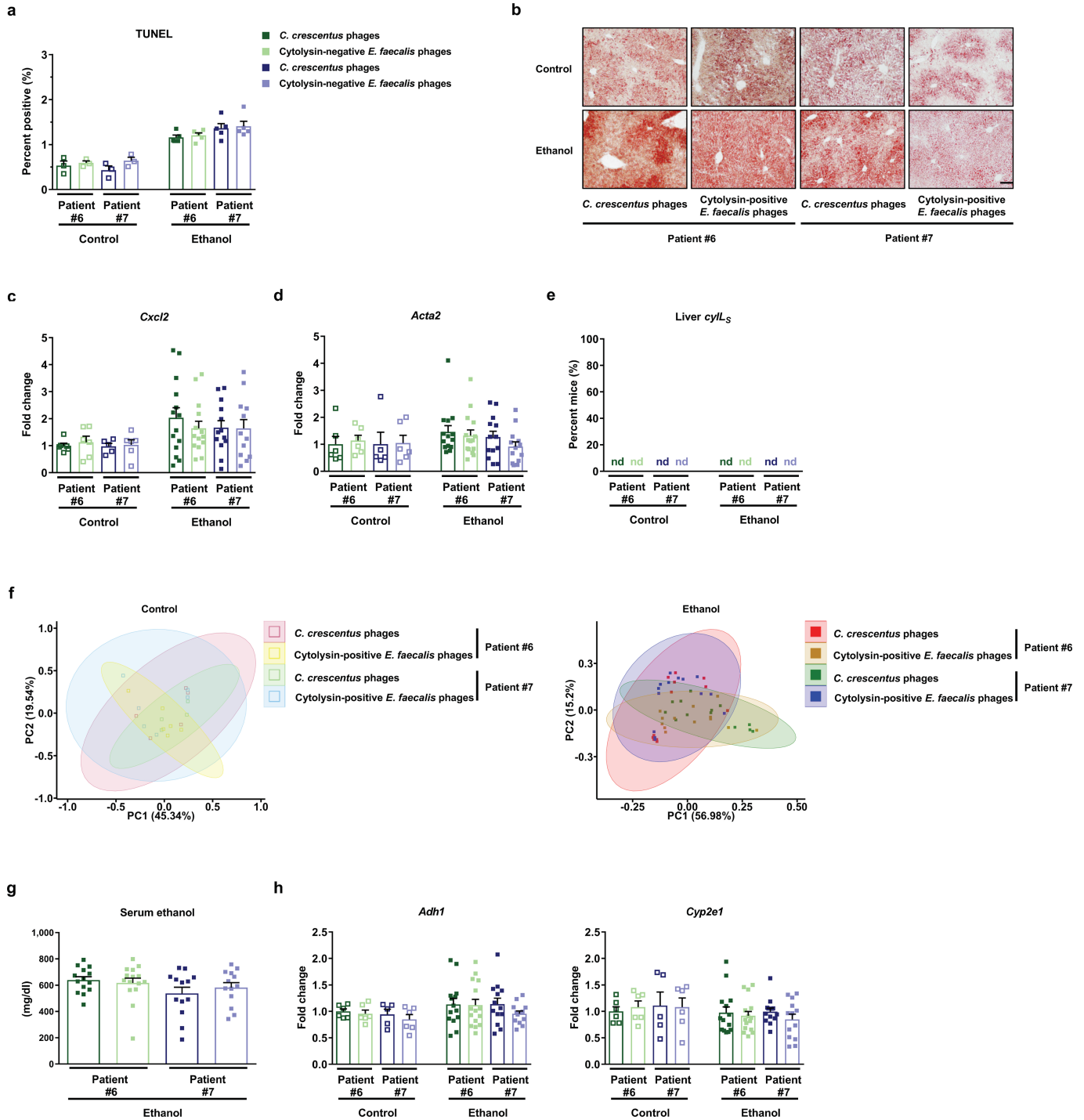
Capsid structural components and assembly	Tail and baseplate assembly	DNA metabolism	Host cell lysis	Other
<p>encapsidation/terminase</p> <p>major capsid</p> <p>portal</p> <p>protease (scaffold protein)</p> <p>other</p>	<p>tail fibers</p> <p>tail component</p> <p>tail measure</p>	<p>DNA polymerase</p> <p>DNA binding</p> <p>DNA recombination</p> <p>salvage of nucleosides and nucleotides</p> <p>DNA restriction/modification</p> <p>nucleotide degradation</p>	<p>endolysin/lysin</p> <p>holin</p>	<p>hypothetical protein</p> <p>intron/intein</p> <p>regulatory</p> <p>tRNA</p>

Extended Data Fig. 8 | See next page for caption.

Article

Extended Data Fig. 8 | Isolation and amplification of phages against non-cytolytic *E. faecalis* strains isolated from patients with alcoholic hepatitis. **a**, BHI agar plates showing phage plaque morphology. **b**, Genetic map of phage genomes. The linear maps are based on nucleotide sequences of the phage genomes and predicted open reading frames. The name and length (in bp) of each genome are indicated to the left of each phage map. Protein-coding sequences are coloured on the basis of functional role categories. Sequences that encode tRNA genes are indicated by a cloverleaf structure. **c**, Phylogenetic tree of *Enterococcus* phages. A whole-genome average nucleotide distance tree was constructed for 73 available *Enterococcus* phage genomes: 54 of these were

from GenBank (denoted by black letters) and 19 were from this study (4 phages against cytolysin-positive *E. faecalis* isolated from mice (shown in blue letters); 7 phages against cytolysin-positive *E. faecalis* isolated from patients with alcoholic hepatitis (shown in pink letters); and 8 phages against cytolysin-negative *E. faecalis* isolated from patients with alcoholic hepatitis (shown in green letters)) with Mash⁴³ using a sketch size of $s = 5000$ and a k -mer size of $k = 12$ and GGRaSP⁵⁹ (Methods). Coloured branches denote specific phage genera or subfamily: Sap6virus, P68virus and *Spounavirinae*. The scale bar represents per cent average nucleotide divergence. All results were generated from at least three independent replicates.



Extended Data Fig. 9 | Phages that target non-cytolytic *E. faecalis* do not reduce ethanol-induced liver disease in gnotobiotic mice. a–h, C57BL/6 germ-free mice were colonized with faeces from two cytolysin-negative patients with alcoholic hepatitis. Transplanted gnotobiotic mice were fed oral isocaloric (control) or chronic-binge ethanol diets and gavaged with control phages against *C. crescentus* (10^{10} PFUs) or a cocktail of four different phages targeting non-cytolytic *E. faecalis* (10^{10} PFUs), 1 day before an ethanol binge. **a**, Percentage of TUNEL-positive hepatic cells. **b**, Representative oil red O-stained liver sections. **c, d**, Hepatic levels of mRNAs that encode the inflammatory cytokine *Cxcl2*, and *Acta2* (a marker of activated hepatic stellate cells). **e**, Proportions of mice that were positive for cytolysin in the liver, measured by qPCR for *cylL_S*. **f**, Faecal samples were collected and 16S rRNA

genes were sequenced. PCoA based on Jaccard dissimilarity matrices found no significant difference in faecal microbiota among mice gavaged with control phages and phages that target cytolysin *E. faecalis* in each group. **g, h**, Serum levels of ethanol and hepatic levels of *Adh1* and *Cyp2e1* mRNAs did not differ significantly among colonized mice after ethanol feeding. Scale bar, 100 μ m. Results are expressed as mean \pm s.e.m. (**a, c, d, g, h**). *P* values were determined by two-way ANOVA with Tukey's post hoc test (**a, c, d, g, h**), two-sided Fisher's exact test followed by FDR procedures (**e**) or PERMANOVA followed by FDR procedures (**f**). All results were generated from at least three independent replicates. The exact group size (*n*) and *P* values for each comparison are listed in Supplementary Table 10.

Reporting Summary

Nature Research wishes to improve the reproducibility of the work that we publish. This form provides structure for consistency and transparency in reporting. For further information on Nature Research policies, see [Authors & Referees](#) and the [Editorial Policy Checklist](#).

Statistics

For all statistical analyses, confirm that the following items are present in the figure legend, table legend, main text, or Methods section.

- | | |
|-----|-----------|
| n/a | Confirmed |
|-----|-----------|
- The exact sample size (n) for each experimental group/condition, given as a discrete number and unit of measurement
 - A statement on whether measurements were taken from distinct samples or whether the same sample was measured repeatedly
 - The statistical test(s) used AND whether they are one- or two-sided
Only common tests should be described solely by name; describe more complex techniques in the Methods section.
 - A description of all covariates tested
 - A description of any assumptions or corrections, such as tests of normality and adjustment for multiple comparisons
 - A full description of the statistical parameters including central tendency (e.g. means) or other basic estimates (e.g. regression coefficient) AND variation (e.g. standard deviation) or associated estimates of uncertainty (e.g. confidence intervals)
 - For null hypothesis testing, the test statistic (e.g. F , t , r) with confidence intervals, effect sizes, degrees of freedom and P value noted
Give P values as exact values whenever suitable.
 - For Bayesian analysis, information on the choice of priors and Markov chain Monte Carlo settings
 - For hierarchical and complex designs, identification of the appropriate level for tests and full reporting of outcomes
 - Estimates of effect sizes (e.g. Cohen's d , Pearson's r), indicating how they were calculated

Our web collection on [statistics for biologists](#) contains articles on many of the points above.

Software and code

Policy information about [availability of computer code](#)

Data collection All biochemical assays were measured using SoftMax Pro 7.0.3; qPCRs were run with StepOnePlus real-time PCR system; Liver histological pictures were taken with DP Controller and DP Manager (Olympus); Phage electronic microscopy pictures were taken using Maxim DL5; Plates were scanned using EPSON 4990 Photo; All pictures were viewed using ImageJ

Data analysis Bacteriophage sequencing and phage tree: Albacore v2.3.4 (ONT), Porechop v0.2.3, Unicycler v0.4.7 pipeline, Pilon v1.22, CLC Genomics Workbench 4.9, NCBI Prokaryotic Genome Annotation Pipeline, in-house PERL script using Xfig, Phage_Finder, MASH program, GGRaSP and APE R-package, iTOL tree viewer
16S sequencing: MOTHUR-based 16S rDNA analysis workflow
E. faecalis genome sequencing and tree: abricate v0.8.10, Prokka, Roary, RAXML, iTOL
Statistical analyses: R statistical software 3.5.1, GraphPad Prism v6.01

For manuscripts utilizing custom algorithms or software that are central to the research but not yet described in published literature, software must be made available to editors/reviewers. We strongly encourage code deposition in a community repository (e.g. GitHub). See the Nature Research [guidelines for submitting code & software](#) for further information.

Data

Policy information about [availability of data](#)

All manuscripts must include a [data availability statement](#). This statement should provide the following information, where applicable:

- Accession codes, unique identifiers, or web links for publicly available datasets
- A list of figures that have associated raw data
- A description of any restrictions on data availability

Raw 16S sequence reads can be found in the NCBI SRA associated with Bioproject PRJNA525701. Bacteriophage raw sequence reads and annotated genomes are

Field-specific reporting

Please select the one below that is the best fit for your research. If you are not sure, read the appropriate sections before making your selection.

Life sciences Behavioural & social sciences Ecological, evolutionary & environmental sciences

For a reference copy of the document with all sections, see [nature.com/documents/nr-reporting-summary-flat.pdf](https://www.nature.com/documents/nr-reporting-summary-flat.pdf)

Life sciences study design

All studies must disclose on these points even when the disclosure is negative.

Sample size	No power analyses or other calculations were used to predetermine sample sizes. Sample sizes were chosen based on prior literature using similar experimental paradigms (Nat Commun. 2017;8:2137; Gut. 2019;68:1504-1515)
Data exclusions	No data were excluded
Replication	In vivo experiments: more than two technical replicates (from different cohorts, on different dates), as well as biological replicates were performed to ensure data reproducibility; In vitro experiments: three independent experiments and also replicates were performed on different dates to ensure data reproducibility. All replications were successful.
Randomization	Mice of similar age and weight were randomly assigned to experimental and control groups.
Blinding	The investigators were not blinded during cell and animal experiment assays.

Reporting for specific materials, systems and methods

We require information from authors about some types of materials, experimental systems and methods used in many studies. Here, indicate whether each material, system or method listed is relevant to your study. If you are not sure if a list item applies to your research, read the appropriate section before selecting a response.

Materials & experimental systems		Methods	
n/a	Involved in the study	n/a	Involved in the study
<input checked="" type="checkbox"/>	<input type="checkbox"/> Antibodies	<input checked="" type="checkbox"/>	<input type="checkbox"/> ChIP-seq
<input checked="" type="checkbox"/>	<input type="checkbox"/> Eukaryotic cell lines	<input checked="" type="checkbox"/>	<input type="checkbox"/> Flow cytometry
<input checked="" type="checkbox"/>	<input type="checkbox"/> Palaeontology	<input checked="" type="checkbox"/>	<input type="checkbox"/> MRI-based neuroimaging
<input type="checkbox"/>	<input checked="" type="checkbox"/> Animals and other organisms		
<input type="checkbox"/>	<input checked="" type="checkbox"/> Human research participants		
<input checked="" type="checkbox"/>	<input type="checkbox"/> Clinical data		

Animals and other organisms

Policy information about [studies involving animals](#); [ARRIVE guidelines](#) recommended for reporting animal research

Laboratory animals	Female and male C57BL/6 mice (age, 9–12 weeks) (strain: wild type, Atp4asl/sl)
Wild animals	No wild animals were involved in the study.
Field-collected samples	No field-collected samples were involved in the study
Ethics oversight	All animal studies were reviewed and approved by the Institutional Animal Care and Use Committee of the University of California, San Diego.

Note that full information on the approval of the study protocol must also be provided in the manuscript.

Human research participants

Policy information about [studies involving human research participants](#)

Population characteristics	Alcoholic hepatitis patients were from multiple centers from United States, Mexico and Europe, with the age ranged from 30 to
----------------------------	---

Population characteristics	75. Alcohol use disorder patients and non-alcoholic controls were from United States and Europe, with the age ranged from 27 to 74. Both genders were included in all populations. Detailed descriptions in Methods, Extended Data Tables 1 and 2
Recruitment	Patients with alcohol use disorder fulfilling the DSM IV criteria (J Abnorm Psychol. 1997;106:545-553) were recruited from an alcohol withdrawal unit in San Diego, USA and Brussels, Belgium where they followed a detoxification and rehabilitation program. Alcoholic hepatitis patients were enrolled from the InTeam Consortium (ClinicalTrials.gov identifier number: NCT02075918) from centers in the USA, Mexico, United Kingdom, France and Spain. Detailed inclusion and exclusion criteria are listed in Methods
Ethics oversight	The protocol was approved by the Ethics Committee of Hôpital Huriez (Lille, France), Universidad Autonoma de Nuevo Leon (Monterrey, México), Hospital Universitari Vall d'Hebron (Barcelona, Spain), King's College London (London, UK), Yale University (New Haven, USA), University of North Carolina at Chapel Hill (Chapel Hill, USA), Weill Cornell Medical College (New York, USA), Columbia University (New York, USA), University of Wisconsin (Madison, USA), VA San Diego Healthcare System (San Diego, USA) and Université Catholique de Louvain (Brussels, Belgium).

Note that full information on the approval of the study protocol must also be provided in the manuscript.